UAB-FT-389
March, 1996
hep-ph/9603441

SUPERSYMMETRIC THREE-BODY DECAYS OF THE TOP QUARK IN THE MSSM

Jaume GUASCH, Joan SOLÀ

Grup de Física Teòrica
and
Institut de Física d'Altes Energies

Universitat Autònoma de Barcelona
08193 Bellaterra (Barcelona), Catalonia, Spain

ABSTRACT

We survey all possible supersymmetric three-body decays of the top quark in the framework of the MSSM and present detailed numerical analyses of the most relevant cases. Although the two-body channels are generally dominant, it is not inconceivable that some or all of our most favourite two-body SUSY candidates could be suppressed. In this event there is still the possibility that some of the available three-body SUSY modes might exhibit a substantial branching fraction and/or carry exotic signatures that would facilitate their identification. Furthermore, in view of the projected inclusive measurement of the top-quark width Γ_t in future colliders, one should have at one's disposal the full second order correction (electroweak and strong) to the value of that parameter in the MSSM. Our analysis confirms that some supersymmetric three-body decays could be relevant and thus contribute to Γ_t at a level comparable to the largest one loop supersymmetric effects on two-body modes recently computed in the literature.

1. Introduction

The era of the top quark has just begun [1]. To a large extent we were prepared to enter the long-announced new epoch and in the meanwhile a tremendous amount of work has piled up on top-quark observables[1]. Yet the extremely rich potential phenomenology and the far-reaching consequences that top-quark dynamics may have on the final picture that will emerge of the Standard Model (SM) of the electroweak and strong interactions definitely demands a new fully fledged wave of theoretical and experimental endeavor in Particle Physics.

The SM has been a most succesful framework to describe the phenomenology of the strong and electroweak interactions for the last thirty years [4]. The top quark itself stood, at a purely theoretical level –namely, on the grounds of requiring internal consistency, such as gauge invariance and renormalizability– as a firm prediction of the SM since the very confirmation of the existence of the bottom quark and the measurement of its weak isospin quantum numbers [5]. Nevertheless, despite all the successes there are still too many questions left unanswered by the SM, especially in connection with the nature of the spontaneous symmetry breaking mechanism (SSB) and the purported existence of the extremely elusive Higgs particle, whether realized as a truly elementary particle or as an effective (composite) field. Due to the huge mass of the top quark, one expects it to be the most preferential fermion to which the Higgs particle should couple. Therefore, top physics is deemed to be the ideal environment for Higgs phenomenology.

Lately the SM has been exposed to an escalate of experimental information potentially challenging some of its predictions to an unprecedented level. We are referring to the long-standing conundrum involving the high precision Z-boson observable R_b and some related observables [6]. The issue about R_b is specially offending, for it seems to consolidate with time–the present day discrepancy with the SM being at the $3.4\,\sigma$ level [7]. Whether this anomaly is linked to an incomplete understanding of the experimental analysis of Z decays into b-quarks, or it can be licitly associated with some sort of physical effects beyond the SM, has not yet been established and at present there is a lot of controversy about it [7]. Be as it may, from the theoretical point of view one is tempted to believe that physics might be taking a definite trend beyond the SM. One possibility is to look at the predictions of the supersymmetric (SUSY) extension of the SM. In this paper we take our chances in favour of the elementary Higgs particle interpretation of the SSB and we adhere to the supersymmetric extension of the SM, more specifically to the Minimal Supersymmetric Standard Model (MSSM) [8]. In particular, there is in the literature quite a big amount of early [9] as well as of very recent SUSY work on R_b [10]-[14]. In some of these works

[1] See e.g. Refs. [2, 3] and references therein.

it is shown that the discrepancies, although they cannot be fully accounted for, at least they can be significantly weakened under suitable conditions [11, 12, 13].

In view of the new wave of SUSY potentialities, it is natural to study all possible phenomenological consequences that may be expected on supersymmetric top-quark physics; after all, the interactions between the top-quark and Higgs sector are doubled in a SUSY framework and one may hope that top-quark physics can be a window to both Higgs bosons and supersymmetric particles. As a first step in this direction one would like to assess the importance of real and virtual SUSY effects on top-quark decays. Here, too, a fairly respectable amount of work is scattered over the literature[2]:

i) Supersymmetric two-body decays of the top quark have been described at the tree level e.g. in Refs.[2], [17]-[21];

ii) Supersymmetric Higgs corrections to the conventional top-quark decay mode $t \to W^+ b$ have been computed in Ref.[22];

iii) Supersymmetric electroweak quantum effects on $t \to W^+ b$ mediated by the roster of genuine supersymmetric particles, such as sleptons, squarks, charginos and neutralinos, have been accounted for in Refs.[23, 24];

iv) Supersymmetric QCD corrections to $t \to W^+ b$ have also been studied in detail in Ref.[25];

v) Supersymmetric QCD effects on the charged Higgs decay of the top quark, $t \to H^+ b$, are generally relevant and can be spectacularly large in favourable regions of the MSSM parameter space [26, 27];

vi) The full plethora of electroweak quantum effects on the unconventional mode $t \to H^+ b$ in the MSSM are also recently available and can be rather significant [16, 28].

We see that on the theoretical side there is a large amount of work ready to be used by experimentalists. Now, what about the prospects for an experimental measurement of these effects?. On the one hand, the measurement of $\Gamma(t \to W^+ b)$ will be carried out at the Tevatron at a level of $\sim 10\%$ and will be further reduced at the LHC. In this respect we remind that the top-quark phenomenology is expected to significantly improve at the Tevatron [3, 29] on the basis of a projected ten-fold increase of the luminosity via the Main Injector and Recycler facilities, together with a $\sim 35\%$ increase of the production cross-section at a $2\,TeV$ running energy (Run II), as compared to the fruitful $1.8\,TeV$ past run (Run I). However, in a hadron machine one aims more at a measurement of specific top-quark production vertices, which are obviously related to the corresponding top-quark partial decay widths. For instance, one of the main goals at the Tevatron for Run II is the measurement of the single top-quark production cross-section [29, 30], which gives essential information on the SM vertex $t\,b\,W$ and, a fortiori, on the value of the

[2]For a review of some of these results, see Refs.[15, 16].

CKM matrix element V_{tb}. In the absence of new physics this measurement is equivalent to a determination of the top quark width. However, in the presence of new interactions beyond the SM, such as e.g. SUSY interactions, one may expect significant changes in the prediction for the cross-section which can be related to the hadronic partial widths of the Higgs bosons of the MSSM [31, 32, 33].

On the other hand, from the point of view of an *inclusive* model-independent measurement of the *total* top-quark width, Γ_t, the future $e^+ e^-$ supercollider should be a better suited machine. In an inclusive measurement, all possible non-SM effects would appear on top of the corresponding SM effects already computed in the literature [34]. As shown in Ref.[35], one expects to be able to measure the top-quark width in $e^+ e^-$ supercolliders at a level of $\sim 4\%$ on the basis of a detailed analysis of both the top momentum distribution and the resonance contributions to the forward-backward asymmetry in the $t\bar{t}$ threshold region.

Clearly, for a consistent treatment of the corrections to the observable Γ_t at second order of perturbation theory (in the strong and electroweak gauge couplings) one should include the tree-level contributions from all possible three-body decays of the top quark in the MSSM. As it happens, the contribution of some of these three-body decays turn out to be comparable to the largest SUSY quantum effects on the two-body channels mentioned above. Furthermore, it could occur that our most cherished SUSY two-body decays are not kinematically allowed or are significantly suppressed in some regions of parameter space. Therefore, supersymmetric three-body decays could be relevant and a detailed study is in order. Such a study is, to our knowledge, missing in the literature and it is precisely the task that we have undertaken in this article. The paper is organized as follows. In Section 2 we present an overview of two-body and three-body decays of the top quark in the MSSM. The Lagrangian interactions relevant to these decays in the MSSM are given in Section 3. The numerical analysis of the various partial widths, with special emphasis on the dominant modes, is detailed in Section 4. Finally, Section 5 is devoted to a discussion of the results, as well as of the possible signatures for the favourite decays, and we deliver our conclusions. An appendix is provided at the end to display some lengthy formulae.

2. Decays of the top quark in the MSSM

The weighted average of the CDF and D0 determinations of the top-quark mass reads as follows [36]:

$$m_t = 175 \pm 9 \ \text{GeV} \,. \tag{1}$$

Due to the large mass of the top quark, there is plenty of phase space available for two-body and multibody decays. Within the minimal SM, the leading standard decay of the

top quark is the "canonical" decay

$$t \to W^+ b\,. \tag{2}$$

The associated partial width is given at the tree-level by

$$\begin{aligned}\Gamma_{SM} \equiv \Gamma(t \to W^+ b) &= \left(\frac{G_F}{8\pi\sqrt{2}}\right) \frac{|V_{tb}|^2}{m_t}\, \lambda^{1/2}(1, \frac{m_b^2}{m_t^2}, \frac{M_W^2}{m_t^2}) \\ &\times [M_W^2(m_t^2 + m_b^2) + (m_t^2 - m_b^2)^2 - 2M_W^4]\,,\end{aligned} \tag{3}$$

where

$$\lambda^{1/2}(1, x^2, y^2) \equiv \sqrt{[1-(x+y)^2][1-(x-y)^2]}\,. \tag{4}$$

Additional standard decays to other quarks are of course possible but, contrary to the canonical decay (in which $V_{tb} \simeq 0.999$, for three generations), they are CKM-suppressed. Numerically, for $m_t = 175$ GeV (and $m_b = 5$ GeV) one has $\Gamma(t \to W^+ b) \simeq 1.54$ GeV, which is very big as compared to $\Lambda_{QCD} \lesssim 300\, MeV$, and therefore the top quark decay is basically a free-quark decay [37]. At this point we should recall that the latest measurements of the canonical branching ratio at the Tevatron still give room enough for top quark decays beyond the SM, namely they could reach $BR(t \to \text{"new"}) \simeq 40\%$ [36].

As for the SUSY two-body decays [2],[17]-[21], the leading modes are the following. On the SUSY-QCD side the top quark can disintegrate, if there is phase space enough, into the lightest stop ($\tilde{t}_1$) and gluino ($\tilde{g}$),

$$t \to \tilde{t}_1\, \tilde{g}\,, \tag{5}$$

and on the SUSY electroweak side we have

$$t \to \tilde{b}_1\, \chi_1^+\,, \tag{6}$$

and

$$t \to \tilde{t}_1\, \chi_1^0\,, \tag{7}$$

where $\tilde{b}_1$ stands for the lightest sbottom and χ_1^+ (χ_1^0) for the lightest chargino (neutralino). In some cases the next-to-lightest neutralinos can also enter and be relevant (see Sections 4-5). Another conspicuous electroweak decay of the top quark in the MSSM involves a supersymmetric charged Higgs in the final state,

$$t \to H^+ b\,. \tag{8}$$

This decay, if kinematically allowed, could be very promising and it has recently been studied up to one-loop order in great detail in Ref.[28]. Numerically, all the two-body SUSY modes can be important as compared to the canonical mode (2) in certain regions

of the MSSM parameter space. We shall compare their contribution with that of the leading three-body decays in Section 4.

Concerning the three-body decays, there are the SM modes where the W^+ is a virtual particle that subsequently goes into lepton or quark final states. However, since the W^+ can be real, the two-body mode (2) followed by the decay of the W^+ as a real particle is overwhelming in the SM. In fact, this is the way in which the top quark has been discovered [1]. Therefore, we are only interested in three-body decays of the top quark in the MSSM other than the three-body SM decays. We shall christen these decays, the SUSY three-body decays of the top quark. In contrast to the SM case, in the MSSM not all of them need to be suppressed as compared to the two-body modes, as we shall see. In an extreme situation, the three-body decays could be the leading SUSY decays of the top quark. There are a fairly big number of them, but in the end only a few can be of some relevance. In the following, and unless stated otherwise, we shall impose the following condition: the relevant three-body decays under study are only those decays in which the virtual particle is heavy enough that the corresponding SUSY two-body decay is kinematically forbidden. Later on we shall relax this condition in some especial cases.

The following decays are essentially ruled out by our conditions or by direct phenomenological constraints:

1. $t \to \tilde{t}_1 W^+ \chi_1^-$: Forbidden by phase space:

$$\begin{array}{rcl} m_{\tilde{t}_1} + M_{\chi_1^-} & < & m_t - M_W \simeq 100 \text{ GeV} \\ m_{\tilde{t}_1} + M_{\chi_1^-} & > & 120 \text{ GeV}\,. \end{array} \tag{9}$$

   where the second relation reflects the recent LEP 130/140 bound on the lightest chargino and sfermion masses [38]

$$m_{\tilde{f}_1}, M_{\chi_1^\pm} \gtrsim 60 \text{ GeV}\,, \tag{10}$$

2. $t \to \tilde{b}_1 \chi_1^0 W^+$: In this case we require

$$\begin{array}{c} m_{\tilde{b}_1} + M_{\chi_1^0} < m_t - M_W \simeq 100 \text{ GeV} \\ m_{\tilde{t}_1} + M_{\chi_1^0} > m_t \\ m_{\tilde{b}_1} + M_{\chi_1^+} > m_t\,, \end{array} \tag{11}$$

   so that

$$\begin{array}{rcl} M_{\chi_1^0} & < & 40 \text{ GeV} \\ M_{\chi_1^+} & > & 80 \text{ GeV} + M_{\chi_1^0}\,, \end{array} \tag{12}$$

   which cannot be fulfilled in the gaugino-higgsino window (μ, M) –see Section 3– of the MSSM parameter space, as we have checked.

3. $t \to \tilde{t}_1 H^{\pm} \chi_1^{\mp}$: Impossible in the MSSM where $m_{H^+} \geq M_W$, and so we cannot fulfil the phase space constraint

$$m_{H^+} < m_t - m_{\tilde{t}_1} - M_{\chi_1^-} \lesssim 60 \text{ GeV}\,, \tag{13}$$

not even in the presence of SUSY radiative corrections, which would lower (only slightly) the charged Higgs boson mass [39].

4. $t \to H^+ \chi_1^0 \tilde{b}_1$, $t \to H^+ \tilde{g} \tilde{b}_1$: For the first process, we have the condition

$$m_{H^+} < m_t - M_{\chi_1^0} - m_{\tilde{b}_1}\,, \tag{14}$$

which forces the charged Higgs mass to be near the lowest limit allowed in the MSSM. For the second, we may admit of both light gluinos $m_{\tilde{g}} = \mathcal{O}(1)$ GeV [40] or heavy gluinos [41],

$$m_{\tilde{g}} \geq 100 \text{ GeV}\,. \tag{15}$$

In the light gluino case, since

$$m_{H^+} < m_t - m_{\tilde{g}} - m_{\tilde{b}_1} \lesssim 120 \text{ GeV}\,, \tag{16}$$

the two-body decay $t \to H^+ b$ would already be allowed. In the heavy gluino scenario, the decay at stake is excluded since it would enforce an unacceptably light charged Higgs:

$$m_{H^+} < m_t - m_{\tilde{g}} - m_{\tilde{b}_1} \lesssim 20 \text{ GeV}\,. \tag{17}$$

5. $t \to \tilde{t}_1 W^+ \chi_1^-$: It would require

$$m_{\tilde{t}_1} + M_{\chi_1^-} < m_t - M_W \simeq 100 \text{ GeV}\,, \tag{18}$$

which is ruled out by eq. (10).

Among the decays in the complete list of SUSY three-body decays of the top-quark in the MSSM which cannot be discarded by trivial arguments, we remark the following:

$$\begin{aligned}
&\textbf{I}. && t \to b\,\tau^+\nu_\tau \\
&\textbf{II}. && t \to h^0\,b\,W^+ \\
&\textbf{III}. && t \to \tilde{b}_a\,W^+\,\tilde{g} \\
&\textbf{IV}. && t \to b\,\chi_\alpha^0\,\chi_i^+ \\
&\textbf{V}. && t \to \tilde{t}_b\,\tilde{b}_a\,\bar{b} \\
&\textbf{VI}. && t \to \tilde{b}_a\,c\,\bar{\tilde{s}}_b \\
&\textbf{VII}. && t \to \tilde{b}_a\,\tau^+\,\bar{\tilde{\nu}}_\tau \\
&\textbf{VIII}. && t \to b\,\tilde{g}\,\chi_i^+ \\
&\textbf{IX}. && t \to b\,\tilde{t}_b\,\bar{\tilde{b}}_a \\
&\textbf{X}. && t \to b\,\tilde{\tau}_a^+\,\tilde{\nu}_\tau\,,
\end{aligned} \tag{19}$$

where for each decay we sum over all sparticle indices allowed by phase space (see Section 4). The decays quoted above do not exhaust the list of potential three-body modes, but the related modes not included in the list are less significant. For instance, decay I above proceeds both via a virtual W^+ and via a virtual charged Higgs boson, H^+. The reason why this decay has been singled out over similar decays involving light quarks, e.g. $t \to b\,u\,\bar{d}$, is because for the latters the charged Higgs couplings to light quarks are suppressed as compared to the coupling to a τ-lepton. As another example, consider decay II. It involves the lightest CP-even SUSY Higgs boson, h^0 [17]. Clearly, two related modes are obtained by replacing h^0 with the heavy CP-even Higgs boson, H^0, or with the CP-odd Higgs boson, A^0. In the first case, the additional decay will obviously be suppressed by phase space; and in the second case, since the charged Higgs H^+ is prescribed to be heavy enough in order to prevent the two-body mode $t \to H^+\,b$ from occurring, it follows from the usual Higgs mass relations in the MSSM [17] that the A^0 must be heavier than h^0, and therefore the corresponding decay is phase-space obstructed.

The Feynman diagrams contributing to the various decays (19) are given in Figs. 1-8. Each process has been thoroughly studied and the main numerical results are provided in Section 4. The upshot of our analysis is that there are a few selected decays in the list (19) that could be of interest. As for the remaining decays, even though they cannot be dismissed by trivial arguments of the sort used in the cases considered before, they eventually prove to be irrelevant.

3. Lagrangian interactions for top quark decays in the MSSM

Although the Lagrangian of the MSSM is well-known [8], it is always useful to project explicitly the relevant pieces and to cast them in a most suitable form for specific purposes. Even with this arrangement, some care is to be exercised in actual calculations, due to the Majorana nature of the neutralinos and the complicated mixing among the various fields. We shall perform our calculations in a mass-eigenstate basis. One goes from the weak-eigenstate basis to the mass-eigenstate basis via appropriate unitary transformations. Two classes of SUSY particles enter our computations: the fermionic partners of the weak-eigenstate gauge bosons and Higgs bosons (called gauginos, $\tilde{B}$, $\tilde{W}$, and higgsinos, $\tilde{H}$, respectively) and on the other hand the scalar partners of quarks and leptons (called squarks, $\tilde{q}$, and sleptons, $\tilde{l}$, respectively, or sfermions, $\tilde{f}$, generically). Among the gauginos we also have the strongly interacting gluinos, $\tilde{g}$, which are the fermionic partners of the gluons. Within the context of the MSSM, we need two Higgs superfield doublets with weak hypercharges $Y_{1,2} = \mp 1$. The (neutral components of the) corresponding scalar Higgs doublets give mass to the down (up) -like quarks through the VEV $< H_1^0 >= v_1$

($< H_2^0 >= v_2$). The ratio

$$\tan\beta = \frac{v_2}{v_1}\,, \tag{20}$$

is a most relevant parameter throughout our analysis.

Due to the "chiral" L-R mixing between weak-eigenstate sfermions of a given flavor,

$$\tilde{q'}_a = \{\tilde{q'}_1 \equiv \tilde{q}_L,\ \tilde{q'}_2 \equiv \tilde{q}_R\}\,, \tag{21}$$

there is a matrix relation with the corresponding squark mass-eigenstates,

$$\tilde{q}_a = \{\tilde{q}_1, \tilde{q}_2\}\,. \tag{22}$$

If we neglect intergenerational mixing, that relation is given by

$$\begin{aligned} \tilde{q'}_a &= \sum_b R^{(q)}_{ab}\,\tilde{q}_b, \\ R^{(q)} &= \begin{pmatrix} \cos\theta_q & \sin\theta_q \\ -\sin\theta_q & \cos\theta_q \end{pmatrix} \qquad (q = t, b)\,, \end{aligned} \tag{23}$$

where we have singled out the third quark generation, (t, b), as a generical fermion-sfermion generation. The rotation matrices in (23) diagonalize stop and sbottom mass matrices:

$$\mathcal{M}^2_{\tilde{t}} = \begin{pmatrix} M^2_{\tilde{t}_L} + m_t^2 + \cos 2\beta(\frac{1}{2} - \frac{2}{3}\,s_W^2)\,M_Z^2 & m_t\,M^t_{LR} \\ m_t\,M^t_{LR} & M^2_{\tilde{t}_R} + m_t^2 + \frac{2}{3}\,\cos 2\beta\,s_W^2\,M_Z^2\,. \end{pmatrix}, \tag{24}$$

$$\mathcal{M}^2_{\tilde{b}} = \begin{pmatrix} M^2_{\tilde{b}_L} + m_b^2 + \cos 2\beta(-\frac{1}{2} + \frac{1}{3}\,s_W^2)\,M_Z^2 & m_b\,M^b_{LR} \\ m_b\,M^b_{LR} & M^2_{\tilde{b}_R} + m_b^2 - \frac{1}{3}\,\cos 2\beta\,s_W^2\,M_Z^2\,, \end{pmatrix}, \tag{25}$$

with

$$M^t_{LR} = A_t - \mu\cot\beta\,, \qquad M^b_{LR} = A_b - \mu\tan\beta\,, \tag{26}$$

μ being the SUSY Higgs mass parameter in the superpotential, $A_{t,b}$ are the trilinear soft SUSY-breaking parameters and the $M_{\tilde{q}_{L,R}}$ are soft SUSY-breaking masses [8]. By $SU(2)_L$-gauge invariance we must have $M_{\tilde{t}_L} = M_{\tilde{b}_L}$, whereas $M_{\tilde{t}_R}$, $M_{\tilde{b}_R}$ are in general independent parameters. With regard to supersymmetric fermionic partners, from the higgsinos and the various gauginos we form the following three sets of two-component Weyl spinors:

$$\Gamma^+_i = \{-i\tilde{W}^+, \tilde{H_2^+}\}\ , \quad \Gamma^-_i = \{-i\tilde{W}^-, \tilde{H_1^-}\}\ , \tag{27}$$

$$\Gamma^0_\alpha = \{-i\tilde{B^0}, -i\tilde{W_3^0}, \tilde{H_2^0}, \tilde{H_1^0}\}\ . \tag{28}$$

These states also get mixed up when the neutral Higgs fields acquire nonvanishing VEV's. The "ino" mass Lagrangian reads

$$\mathcal{L}_M = - < \Gamma^+|\mathcal{M}|\Gamma^- > -\frac{1}{2} < \Gamma^0|\mathcal{M}^0|\Gamma^0 > + h.c.\ , \tag{29}$$

where the charged and neutral gaugino-higgsino mass matrices $\mathcal{M}, \mathcal{M}^0$ are also well-known; in our notation they are given explicitly in Ref.[23], where we remark the presence of the parameter μ introduced above and of the soft SUSY-breaking Majorana masses M and M', usually related as $M'/M = (5/3)\,\tan^2\theta_W$. The corresponding four-component mass-eigenstate spinors, the so-called charginos and neutralinos, are the following[3]:

$$\Psi_i^+ = \begin{pmatrix} U_{ij}\Gamma_j^+ \\ V_{ij}^*\bar{\Gamma}_j^- \end{pmatrix} \quad , \quad \Psi_i^- = C\bar{\Psi}_i{}^{+T} = \begin{pmatrix} V_{ij}\Gamma_j^- \\ U_{ij}^*\bar{\Gamma}_j^+ \end{pmatrix} , \tag{30}$$

and

$$\Psi_\alpha^0 = \begin{pmatrix} N_{\alpha,\beta}\Gamma_\beta^0 \\ N_{\alpha,\beta}^*\bar{\Gamma}_\beta^0 \end{pmatrix} = C\bar{\Psi}_\alpha^{0T} . \tag{31}$$

where the matrices U, V, N are defined through

$$U^*\mathcal{M}V^\dagger = diag\{M_1, M_2\} \quad , \quad N^*\mathcal{M}^0N^\dagger = diag\{M_1^0, ...M_4^0\} . \tag{32}$$

With the help of these matrices, the following interaction vertices appear in the SUSY three-body decays of the top quark (after rewriting them in the mass-eigenstate basis for all sparticles):

- fermion–sfermion–(chargino or neutralino):

$$\begin{aligned} \mathcal{L} \;=\; & -g\tilde{t}_a^*\,\bar{\chi}_i^-\left(A_{+ai}^{\;\;t}\epsilon_i P_L + A_{-ai}^{\;\;t}P_R\right)b \\ & -g\tilde{b}_a^*\,\bar{\chi}_i^+\left(A_{+ai}^{\;\;b}P_L + A_{-ai}^{\;\;b}\epsilon_i P_R\right)t \\ & -\tfrac{g}{\sqrt{2}}\tilde{t}_a^*\,\bar{\chi}_\alpha^0\left(A_{+a\alpha}^{(0)t}P_L + A_{-a\alpha}^{(0)t}\epsilon_\alpha P_R\right)t \\ & +\tfrac{g}{\sqrt{2}}\tilde{b}_a^*\,\bar{\chi}_\alpha^0\left(A_{+a\alpha}^{(0)b}P_L + A_{-a\alpha}^{(0)b}\epsilon_\alpha P_R\right)b \\ & +\text{ h.c.} \end{aligned} \tag{33}$$

Here $P_{L,R} = \frac{1}{2}\,(1 \mp \gamma^5)$ are the chiral projectors, and we have defined the following coupling matrices:

$$\begin{cases} A_{+ai}^{\;\;t} &= R_{1a}^{(t)*}U_{i1}^* - \lambda_t R_{2a}^{(t)*}U_{i2}^* \\ A_{-ai}^{\;\;t} &= -R_{1a}^{(t)*}\lambda_b V_{i2} \\ A_{+ai}^{\;\;b} &= R_{1a}^{(b)*}V_{i1}^* - \lambda_b R_{2a}^{(b)*}V_{i2}^* \\ A_{-ai}^{\;\;b} &= -R_{1a}^{(b)*}\lambda_t U_{i2} \\ A_{+a\alpha}^{(0)t} &= R_{1a}^{(t)*}\left(N_{\alpha2}^* + Y^L\tan\theta_W N_{\alpha1}^*\right) + R_{2a}^{(t)*}\sqrt{2}\lambda_t N_{\alpha3}^* \\ A_{-a\alpha}^{(0)t} &= R_{1a}^{(t)*}\sqrt{2}\lambda_t N_{\alpha3} + R_{2a}^{(t)*}Y_t^R\tan\theta_W N_{\alpha1} \\ A_{+a\alpha}^{(0)b} &= R_{1a}^{(b)*}\left(N_{\alpha2}^* - Y^L\tan\theta_W N_{\alpha1}^*\right) - R_{2a}^{(b)*}\sqrt{2}\lambda_b N_{\alpha4}^* \\ A_{-a\alpha}^{(0)b} &= -R_{1a}^{(b)*}\sqrt{2}\lambda_b N_{\alpha4} - R_{2a}^{(t)*}Y_b^R\tan\theta_W N_{\alpha1} , \end{cases} \tag{34}$$

where Y^L and $Y_{t,b}^R$ are respectively the weak hypercharges of the left-handed $SU(2)_L$ doublet and right-handed singlet fermion-sfermion partners within the chiral supermultiplet. The potentially significant Yukawa couplings are contained in the

[3]We use the notation of Ref.[23], namely, first Latin indices a,b,...=1,2 are reserved for sfermions, middle Latin indices i,j,...=1,2 for charginos, and first Greek indices $\alpha, \beta, ... = 1, 2, ..., 4$ for neutralinos.

following ratios with respect to the $SU(2)_L$ gauge coupling:

$$\lambda_t \equiv \frac{h_t}{g} = \frac{m_t}{\sqrt{2}\, M_W\, \sin\beta} \quad , \quad \lambda_b \equiv \frac{h_b}{g} = \frac{m_b}{\sqrt{2}\, M_W\, \cos\beta}\,. \tag{35}$$

In the previous formulae we have changed the chargino-neutralino basis from $\{\Psi_i^\pm, \Psi_\alpha^0\}$ to $\{\chi_i^\pm, \chi_\alpha^0\}$ and in the latter we have introduced the coefficients ϵ_i and ϵ_α. The reason for this change of basis is because in the numerical analysis we use real, instead of complex, diagonalization matrices U, V, N for charginos and neutralinos. Thus we have to compensate for the minus signs that may appear in the list of mass eigenvalues by introducing the ϵ parameters. For instance, for chargino masses we set, for each $i = 1, 2$:

$$M_i = \epsilon_i |M_i|\,. \tag{36}$$

In this formalism the physical chargino, $\chi_i^\pm$, is not always the the mass-eigenstate spinor defined in eq.(30), but

$$\chi_i^\pm = \begin{cases} \Psi_i^\pm & \text{if} \quad \epsilon_i = 1 \\ \pm\gamma_5 \Psi_i^\pm & \text{if} \quad \epsilon_i = -1\,. \end{cases} \tag{37}$$

This is equivalent to replace

$$\begin{aligned} \Psi_i^+ \quad &\rightarrow \quad \chi_i^+ \equiv (P_R + \epsilon_i P_L)\, \Psi_i^+ \\ \Psi_i^- \quad &\rightarrow \quad \chi_i^- \equiv (P_L + \epsilon_i P_R)\, \Psi_i^- = C\bar{\chi_i}^{+T}\,. \end{aligned} \tag{38}$$

Indeed, with this proviso the new kinetic Lagrangian for the chargino has always the correct sign:

$$\mathcal{L}_K = \bar{\Psi}_i^+ \,(i\partial\!\!\!/ - M_i)\, \Psi_i^+ = \bar{\chi}_i^+ \,(i\partial\!\!\!/ - |M_i|)\, \chi_i^+\,. \tag{39}$$

We proceed similarly with neutralinos, for each $\alpha = 1, ..., 4$:

$$M_\alpha = \epsilon_\alpha |M_\alpha|\,, \tag{40}$$

and

$$\Psi_\alpha^0 \rightarrow \chi_\alpha^0 \equiv (P_R + \epsilon_\alpha P_L)\, \Psi_\alpha^0\,. \tag{41}$$

Notice, however, that in the real formalism just sketched the physical neutralinos are no longer Majorana particles in general (Cf. eq.(31)), since they satisfy

$$\chi_\alpha^{0c} = \mathcal{C}\bar{\chi}_\alpha^{0T} = \epsilon_\alpha \chi_\alpha^0\,. \tag{42}$$

Once these definitions have been made one has to propagate them carefully over all the interaction terms and keep track of the ϵ parameters [4]. There are a few

[4] This procedure is equivalent to the one defined in Refs.[17, 42]. We have corrected some sign errors and some missing ϵ's in the Feynman rules given in these references.

more or less known subtleties related to Majorana particles in connection with the ϵ formalism which are worth remembering. Thus e.g. take a generical Lagrangian interaction involving a neutral Higgs and two neutralinos:

$$\begin{aligned} \mathcal{L} &= gH^0\bar{\chi}^0_\gamma\epsilon_\delta\Gamma_{\gamma\delta}P_L\chi^0_\delta + \text{ h.c.} \\ &= gH^0\bar{\chi}^0_\gamma\left(\epsilon_\delta\Gamma_{\gamma\delta}P_L + \epsilon_\gamma\Gamma^*_{\delta\gamma}P_R\right)\chi^0_\delta\,. \end{aligned} \tag{43}$$

Since χ^0_α can be created or destroyed by any of the fermionic field operators appearing in the Lagrangian, for a term with fixed indices α and β on eq.(43) we have

$$\begin{aligned} \mathcal{L}_{\alpha\beta} &= gH^0\bar{\chi}^0_\alpha\left(\epsilon_\beta\Gamma_{\alpha\beta}P_L + \epsilon_\alpha\Gamma^*_{\beta\alpha}P_R\right)\chi^0_\beta \\ &\quad + gH^0\bar{\chi}^0_\beta\left(\epsilon_\alpha\Gamma_{\beta\alpha}P_L + \epsilon_\beta\Gamma^*_{\alpha\beta}P_R\right)\chi^0_\alpha\,. \end{aligned} \tag{44}$$

Therefore, using eq.(42) and the usual properties of the charge conjugation matrix, we may rearrange the two terms in (44) as follows:

$$\mathcal{L}_{\alpha\beta} = gH^0\bar{\chi}^0_\alpha\left(\epsilon_\beta(\Gamma_{\alpha\beta}+\Gamma_{\beta\alpha})P_L + \epsilon_\alpha(\Gamma^*_{\beta\alpha}+\Gamma^*_{\alpha\beta})P_R\right)\chi^0_\beta\,. \tag{45}$$

Notice that, for virtual particles, the rule (38) just entails the following replacement in the numerator of the chargino propagator:

$$\not{p} + |M_i| \longrightarrow \not{p} + \epsilon_i|M_i| = \not{p} + M_i\,, \tag{46}$$

and similarly for neutralinos, so that one can use real matrices U, V, N together with positive or negative mass eigenvalues, since the ϵ's just cancel out [23]. For real sparticles in the final state, a similar thing occurs for the square of the various amplitudes involved in the top quark decay, but here one has to keep track of the ϵ's anyway since they may play a crucial role in the computation of the interference terms. In our formulae we shall nevertheless maintain the original complex notation so that one can either use complex mixing matrices and forget altogether about ϵ's or, alternatively, to keep the ϵ's and consider that all the coupling matrices are real.

- quark–squark–gluino:

$$\mathcal{L} = -\frac{g_s}{\sqrt{2}}\tilde{q}^*_{a,k}\,\bar{\tilde{g}}_r\,(\lambda^r)_{k,l}\left(R^{(q)*}_{1a}P_L - R^{(q)*}_{2a}P_R\right)q_l + \text{ h.c.} \tag{47}$$

where λ^r are the Gell-Mann matrices. This is just the SUSY-QCD Lagrangian written in the squark mass-eigenstate basis.

- squark–squark–Higgs:

$$\mathcal{L} = -\frac{g}{\sqrt{2}M_W}\tilde{t}^*_c\tilde{b}_d\,R^{(t)*}_{ac}R^{(b)}_{bd}\,g_{ab}H^+ + \text{ h.c.} \tag{48}$$

where we have introduced the coupling matrix

$$g_{ab} = \begin{pmatrix} M_W^2\sin 2\beta - (m_b^2\tan\beta + m_t^2\cot\beta) & -m_b\,(\mu + A_b\tan\beta) \\ -m_t\,(\mu + A_t\cot\beta) & -m_t m_b\,(\tan\beta + \cot\beta) \end{pmatrix}. \tag{49}$$

- chargino–neutralino–Higgs:

$$\mathcal{L} = -gH^+ \,\bar{\chi}_i^+ \left(\sin\beta\, Q_{\alpha i}^{R*}\epsilon_\alpha P_L + \cos\beta\, Q_{\alpha i}^{L*}\epsilon_i P_R\right)\chi_\alpha^0 + \text{ h.c.}\,, \tag{50}$$

with

$$\left\{\begin{array}{lcl} Q_{\alpha i}^L &=& U_{i1}^* N_{\alpha 3}^* + \frac{1}{\sqrt{2}}\left(N_{\alpha 2}^* + \tan\theta_W N_{\alpha 1}^*\right) U_{i2}^* \\ Q_{\alpha i}^R &=& V_{i1} N_{\alpha 4} - \frac{1}{\sqrt{2}}\left(N_{\alpha 2} + \tan\theta_W N_{\alpha 1}\right) V_{i2}\,. \end{array}\right. \tag{51}$$

- Gauge interactions: In our calculation we only need the sparticle interactions with the $W^\pm$:

  - quarks:

$$\mathcal{L} = \frac{g}{\sqrt{2}}\,\bar{t}\gamma^\mu P_L b\, W_\mu^+ + \text{ h.c.} \tag{52}$$

  - squarks:

$$\mathcal{L} = i\frac{g}{\sqrt{2}} R_{1b}^{(t)*} R_{1a}^{(b)} W_\mu^+ \tilde{t}_b^* \overleftrightarrow{\partial^\mu}\, \tilde{b}_a + \text{ h.c.} \tag{53}$$

  - charginos and neutralinos:

$$\mathcal{L} = g\,\bar{\chi}_\alpha^0 \gamma^\mu \left(C_{\alpha i}^L \epsilon_\alpha \epsilon_i P_L + C_{\alpha i}^R P_R\right)\chi_i^+ W_\mu^- + \text{ h.c.} \tag{54}$$

$$\left\{\begin{array}{lcl} C_{\alpha i}^L &=& \frac{1}{\sqrt{2}} N_{\alpha 3} U_{i2}^* - N_{\alpha 2} U_{i1}^* \\ C_{\alpha i}^R &=& -\frac{1}{\sqrt{2}} N_{\alpha 4}^* V_{i2} - N_{\alpha 3}^* V_{i1}\,. \end{array}\right. \tag{55}$$

There are of course some additional interactions that can be involved in the SUSY three-body decays of the top quark, such as the various quark-quark-higgs vertices, and also the vertices involving one gauge boson and two higgses or viceversa. However, they are pretty well-known and we shall not quote them here [17].

4. Numerical analysis

As mentioned in the preliminary survey of Section 2, among the potentially relevant SUSY three-body modes (19), only a few result in sizeable corrections to the top quark width. The relevant modes are defined to be as those that can give a contribution

$$\frac{\delta\Gamma^{SUSY}}{\Gamma_{SM}} \gtrsim 1\%\,, \tag{56}$$

with respect to the the canonical width (3) of the top quark in the SM. For comparison, let us recall the size of the one-loop corrections to the canonical decay (2) –these quantum corrections being of the same order in perturbation theory as our three-body decays at the tree-level. The corresponding SM electroweak corrections lie in the ballpark of 1.5% (in the G_F-scheme) [34] for the present values of the top-quark mass, whereas the QCD corrections are of order $-(8-9)\%$ [34] and are essentially independent of m_t. Our analysis

shows that the SUSY three-body decays on eq.(19) that most likely could fulfil condition (56) are the modes I, IV, VIII, IX, X.

As an independent set of SUSY inputs we introduce a similar tuple of parameters as in the numerical analyses of Refs. [11]-[13], specifically:

$$(\tan\beta, m_{H^+}, \mu, M, m_{\tilde{g}}, m_{\tilde{b}_1}, m_{\tilde{t}_1}, M^b_{LR}, M^t_{LR})\,. \tag{57}$$

For the full numerical analysis of the ten decays (19) we have produced several hundred plots in order to explore all the relevant peculiarities of the 9-dimensional parameter space of eq. (57) [44]. In what follows we limit ourselves to report on the main results obtained under more simplified assumptions which do not alter the maximal rates expected. In particular, throughout all our numerical analysis we use a representative set of inputs which is non-critical, i.e. such that our results behave smoothly under variations around these values. The simplifying assumptions mentioned above are the following. We shall assume that the mixing angle in the stop sector is $\theta_t = \pi/4$. In the sbottom sector, where mixing effects are more unlikely, we fix $M^b_{LR} = 0$ and $m_{\tilde{b}_1} = m_{\tilde{b}_2} \equiv m_{\tilde{b}}$. With these settings the stop mass eigenvalues $m_{\tilde{t}_{1,2}}$ are determined and hence a more restricted set of parameters is obtained than the general set (57). In most processes, this suffices. Notwithstanding, we shall come back to the general set (57) later on for some of the most promising decays.

Apart from the phenomenological limits on the various sparticle masses mentioned above, we shall explore the crucial parameter $\tan\beta$, eq.(20), within the range

$$0.5 \lesssim \tan\beta \lesssim 70\,, \tag{58}$$

which is fixed by the perturbative domain of the Yukawa couplings (35). Apart from the well established SM inputs [43], we adopt the following for our numerical analysis:

$$\begin{array}{c} m_b = 5 \text{ GeV} \\ m_t = 175 \text{ GeV} \\ V_{tb} = 0.999 \\ \alpha_s(m_t) = 0.11\,. \end{array} \tag{59}$$

- **Decay I**: There are two Feynman diagrams contributing to this process (Cf. Fig.1). Only two parameters from the general set (57) are needed in this case, namely

$$(\tan\beta, m_{H^+})\,. \tag{60}$$

  Diagram (a) in Fig.1 is the conventional diagram, whereas diagram (b) gives the extra Higgs contribution, which is determined by the strength of the Yukawa couplings given on eq.(35) with m_τ in place of m_b. Notice that in this case the charged Higgs

need not to be supersymmetric but just the charged member of a general two-Higgs doublet model of type II [17]. Since $m_\tau > m_q$ for any light quark, in the region of $\tan\beta > 1$ we do not consider the similar decays in which (ν_τ, τ^+) is replaced with $(u, \bar{d})$ or $(c, \bar{s})$. On imposing the condition that the two-body decay $t \to H^+ b$ is not kinematically permissible, we study the three-body decay only for Higgs masses

$$m_{H^+} > m_t - m_b \,. \tag{61}$$

Since we aim at a departure from the SM contribution, we define the quantity

$$\delta_I = \frac{\Gamma\left(t \to b\nu_\tau\tau^+\right) - \Gamma\left(t \to bW^{+*} \to b\nu_\tau\tau^+\right)}{\Gamma\left(t \to bW^{+*} \to b\nu_\tau\tau^+\right)} \,, \tag{62}$$

and plot contour lines of δ_I in the plane (60) under the condition (61). The result is displayed in Fig. 9. Notice that $\Gamma\left(t \to b\nu_\tau\tau^+\right)$ on eq.(62) is computed from the sum of the two amplitudes in Fig.1, whereas $\Gamma\left(t \to bW^{+*} \to b\nu_\tau\tau^+\right)$ includes the first amplitude only. It is seen from Fig. 9 that corrections of a few percent are possible at high $\tan\beta$. In the low $\tan\beta < 1$ region, the decay under study is inefficient since the τ-lepton Yukawa coupling becomes very depleted. In spite of the fact that in this region of $\tan\beta$ the alternative decay $t \to b\, c\bar{s}$ can give contributions of order 1%, this channel would be much more difficult to separate from the background.

The dominance of the the semileptonic channel for $\tan\beta > \mathcal{O}(1)$ occurs for both real or virtual Higgs decays. For real decays, we have

$$\begin{aligned} \frac{\Gamma(H^+ \to \tau^+\nu_\tau)}{\Gamma(H^+ \to c\bar{s})} &= \frac{1}{3}\left(\frac{m_\tau}{m_c}\right)^2 \frac{\tan^2\beta}{(m_s^2/m_c^2)^2\tan^2\beta + \cot^2\beta} \\ &\to \frac{1}{3}\left(\frac{m_\tau}{m_s}\right)^2 > 10 \qquad \left(\text{for } \tan\beta > \sqrt{m_c/m_s} \gtrsim 3\right). \end{aligned} \tag{63}$$

The identification of the τ mode could be a matter of measuring a departure from the universality prediction between all lepton channels. Fortunately, τ-identification is possible at Tevatron [45]; and the feasibility of tagging the excess of events with one isolated τ-lepton as compared to events with an additional lepton has been substantiated by studies of the LHC collaborations [46]. It has recently been shown that it should be fairly easy to discriminate between the W-daughter τ's and the $H^\pm$-daughter τ's by just looking at the opposite states of τ polarization resulting from the $W^\pm$ and $H^\pm$ decays; the two polarization states can be distinguished by measuring the charged and neutral contributions to the 1-prong τ-jet energy (even without identifying the individual meson states) [47].

- **Decay II**: There are four Feynman diagrams contributing to this decay, and they are displayed in Fig.2. In principle, h^0 in these diagrams could be replaced with any

of the neutral MSSM higgses. However, the following relations must hold simultaneously

$$\begin{array}{rcl} m_{h^0} & < & m_t - m_b - M_W \\ m_{H^+} & > & m_t - m_b \,. \end{array} \tag{64}$$

in order to allow the three-body decay and at the same time to forbid the two-body charged Higgs mode (8) involved in one of the amplitudes. In the MSSM, the second relation implies (at the tree-level) [17] that $m_{A^0} > 155$ GeV, and since the heavy CP-even Higgs satisfies $m_{H^0} > M_Z$, the relations (64) can only be fulfilled by the lightest CP-even Higgs h^0. Again the only two parameters involved are those in eq.(60), since the mixing angle, α, between the CP-even higgses is not independent in the MSSM [17]. Unfortunately, a fully fledged calculation of the diagrams in Fig.2 yields a disappointingly small contribution, as seen in Fig.10. The reason for it is the following. The potentially relevant neutral Higgs Yukawa couplings $h^0\,t\,t$ and $h^0\,b\,b$ in Figs. 2a and 2c are proportional to $\cos\alpha/\sin\beta$ and $\sin\alpha/\cos\beta$, respectively [17]. Since m_{A^0} is assumed to be large, then α goes to zero or to $-\pi/2$ depending on whether $\tan\beta$ is large or small, respectively. In neither case these Yukawa couplings become enhanced with respect to the gauge coupling. The other potentially relevant interaction is the charged Higgs vertex $H^+\,t\,b$ in Fig. 2b, which is sensitive to both Yukawa couplings on eq.(35) and is independent of α [17]. Unfortunately, this vertex is also rendered ineffective in the present conditions, since its behaviour at large and small $\tan\beta$ is compensated for by the opposite behaviour of the companion vertex $W^+\,H^+\,h^0$ in the same diagram, which is proportional to $\cos(\alpha-\beta) \to 0$. In the end there is a balance between the four diagrams giving rise to a maximum near $\tan\beta = 1.5$, although the resulting contribution with respect to the canonical decay is rather meagre, namely

$$\delta_{II} = \frac{\Gamma(t \to h^0\,b\,W^+)}{\Gamma_{SM}} < 3 \times 10^{-4}\,, \tag{65}$$

making the observation of this process essentially hopeless.

- **Decay III**: The corresponding Feynman diagrams are in Fig.3 [5]. Obviously, this decay can only proceed within the context of the so-called light gluino scenario $m_{\tilde{g}} = \mathcal{O}(1)$ GeV [40], since for heavy gluinos the usual bound (15) prevents the decay from occurring. With $m_{\tilde{g}}$ assumed to be negligible, we are left with the additional conditions

$$\begin{array}{c} m_{\tilde{b}} < m_t - M_W \\ m_{\tilde{t}_1} > m_t \,, \end{array} \tag{66}$$

[5] We remark that in all our Feynman diagrams indices for virtual sparticles are understood to be summed over.

where the second relation is to guarantee that the two-body decay (5) does not take place. The relevant subset of parameters in the present instance is

$$(\tan\beta, m_{\tilde{g}}, m_{\tilde{b}}, M^t_{LR})\,. \tag{67}$$

The numerical analysis is presented for a light gluino mass $m_{\tilde{g}} = 1$ GeV and fixed $\tan\beta = 1$ since small values of $\tan\beta$ are preferred. The results are basically the same within the light gluino range $m_{\tilde{g}} = (1-10)$ GeV and are rather insensitive to allowed values of M^t_{LR} below m_t, so we have set $M^t_{LR} = 0$. In Fig. 11 we display the contribution of the LH sbottom final state. For LH sbottom masses respecting the absolute LEP bound (10), we find

$$\delta_{III} = \frac{\Gamma(t \to \tilde{b}_a\, W^+\, \tilde{g})}{\Gamma_{SM}} < 0.1\,, \tag{68}$$

which is well below the limit (56) and therefore is too small. The yield from the RH sbottom final state is even smaller ($< 10^{-5}$) due to the helicity flip at the bottom line in Fig. 3a.

- **Decay IV**:This process is rather complex since it involves four Feynman diagrams (see Fig. 4) and the following parameters:

$$(\tan\beta, m_{H^+}, \mu, M, m_{\tilde{b}}, M^t_{LR})\,. \tag{69}$$

The simultaneous conditions to be required in order that this decay is possible while the two-body modes (6)-(8) are forbidden are the following:

$$\begin{array}{c} M_{\chi^0_\alpha} + M_{\chi^+_i} + m_b < m_t \\ m_{H^+} > m_t - m_b \\ M_{\chi^0_1} + m_{\tilde{t}} > m_t \\ M_{\chi^+_1} + m_{\tilde{b}} > m_t\,. \end{array} \tag{70}$$

Notice that in practice the handling of these relations has to be carried out numerically since our inputs (69) are not given directly in terms of the chargino and neutralino masses. Therefore one has to diagonalize the chargino and neutralino mass matrices on eq.(29) and look for regions in the higgsino-gaugino parameter space (μ, M) where the relations (70) are met. We have checked that the maximum contribution of this decay is obtained near the phenomenological boundaries defined by the condition (10). In Fig. 12 we plot the ratio

$$\delta_{IV} = \frac{\Gamma(t \to b\, \chi^0_1\, \chi^+_1)}{\Gamma_{SM}}\,, \tag{71}$$

as a function of $\tan\beta$ for a typical (μ, M) boundary point corresponding to $m_{\chi^+_1} =$ 60 GeV. We see that at high $\tan\beta$ there are significant enhancements of δ_{IV} which

could boost this quantity up to a value $\sim 6-8\%$, i.e. up to the level of the conventional QCD corrections to the canonical decay. We have checked that the total effect from the next-to-lightest charginos and neutralinos allowed by phase space amounts to an additional contribution of 0.6% in the high $\tan\beta$ region. In view of these results, it follows that this three-body mode could be relevant.

- **Decay V**: Three Feynman diagrams contribute to this decay (see Fig. 5) and the parameters involved read

$$(\tan\beta, \mu, M, m_{\tilde{g}}, m_{\tilde{b}}, M^t_{LR})\,, \tag{72}$$

which are limited by the conditions

$$\begin{array}{c} m_{\tilde{t}} < m_t - m_b - m_{\tilde{b}} \\ m_{\tilde{g}} > m_t - m_{\tilde{t}} \\ M_{\chi_1^0} + m_{\tilde{t}} > m_t \\ M_{\chi_1^+} + m_{\tilde{b}} > m_t\,. \end{array} \tag{73}$$

Since gluinos can either be very light, viz. of $\mathcal{O}(1)$ GeV, or at least as heavy as 100 GeV, the second condition above enforces a heavy gluino scenario. Within our current set of hypotheses we exclude a heavy stop and a light gluino since the (degenerate) sbottoms would be heavy, too, and the phase space would be exhausted. In Fig. 13 we present a "lattice plot" sampling [11] of the 6-tuple (72), separately for LH and RH sbottoms. We see that the ratio

$$\delta_V = \frac{\Gamma(t \to \tilde{t}_1\, \tilde{b}_a\, \bar{b})}{\Gamma_{SM}}\,, \tag{74}$$

shows the highest cumulative number of points for values $\delta_V < 0.2\%$ whereas higher values get only a few number of spots.

- **Decay VI**: This decay is particularly simple, for it admits a single Feynman diagram (Fig. 6a). The input parameters are

$$(\tan\beta, \mu, M, m_{\tilde{b}}, m_{\tilde{s}})\,, \tag{75}$$

under the conditions

$$\begin{array}{c} 2\, m_{\tilde{b}} < m_t - m_c \\ m_{\tilde{b}} + M_{\chi_1^+} > m_t\,, \end{array} \tag{76}$$

where we assume $m_{\tilde{b}} = m_{\tilde{s}}$. Thus we are led to an scenario of heavy charginos and relatively light squarks. In Fig. 14a we display the ratio

$$\delta_{VI} = \frac{\Gamma(t \to \tilde{b}_a\, c\, \bar{\tilde{s}}_b)}{\Gamma_{SM}}\,, \tag{77}$$

for the different combinations of chiral species of squarks. Contributions of order $\delta_{VI} \simeq 1\%$ obtain for $\tan\beta \lesssim 0.6$, i.e. near the lower limit (58).

- **Decay VII**: This decay is similar to the previous one (see Fig. 6b), but it involves τ-sleptons in the final state. Thus the inputs are

$$(\tan\beta, \mu, M, m_{\tilde{b}}, m_{\tilde{\tau}})\,, \tag{78}$$

bounded as follows

$$\begin{array}{c} m_{\tilde{b}} + m_{\tilde{\tau}} < m_t \\ m_{\tilde{b}} + M_{\chi_1^+} > m_t\,. \end{array} \tag{79}$$

The relevant ratio

$$\delta_{VII} = \frac{\Gamma(t \to \tilde{b}_a\, \nu_\tau\, \tilde{\tau}_b^+)}{\Gamma_{SM}}\,, \tag{80}$$

is analyzed in Fig. 14b for the different combinations of chiral species of staus and sbottoms. In the present instance, where sleptons are around, we assume a corresponding mass matrix with the same simplified structure as that of the sbottom mass matrix. Therefore, the LH and RH staus are degenerate, with a common mass $m_{\tilde{\tau}} \gtrsim 95$ GeV, which guarantees $m_{\tilde{\nu}} \gtrsim 40$ GeV – as required by the data on the invisible Z-width [6]. In these conditions, it is seen from Fig. 14b that $\delta_{VII} \simeq 1\%$ is achieved for $\tan\beta$ very near the two extreme values of the allowed interval (58), but only at the expense of a rather light chargino $M_{\chi_1^+} \simeq 50$ GeV, which is still permitted if it is almost degenerate with the lightest neutralino [38].

- **Decay VIII**: This decay is related to number IV in that a gluino substitutes for a neutralino. The number of Feynman amplitudes stays the same (Cf. Fig. 7) and the relevant tuple of independent parameters can be chosen as follows:

$$(\tan\beta, m_{\tilde{g}}, \mu, M, m_{\tilde{t}}, M_{LR}^t)\,, \tag{81}$$

being subdued by the conditions

$$\begin{array}{c} M_{\chi_i^+} + m_{\tilde{g}} < m_t - m_b \\ m_{\tilde{t}} + m_{\tilde{g}} > m_t \\ m_{\tilde{b}} + M_{\chi_i^+} > m_t\,, \end{array} \tag{82}$$

whose meaning should by now be pretty obvious. In contrast to decay V, both the light and heavy gluino scenario is permissible in the present instance. In the first case (light gluinos), a heavy stop and a heavy chargino could coexist with a relatively light sbottom, while in the second case (heavy gluinos) a light stop is tolerated at the expense of heavy sbottoms. The numerical analysis of the quantity

$$\delta_{VIII} = \frac{\Gamma(t \to b\, \tilde{g}\, \chi_i^+)}{\Gamma_{SM}}\,, \tag{83}$$

shows that in the heavy gluino scenario the contributions are well below 1% and we do not show explicit plots. In contrast, for light gluinos we see in Fig.15 that δ_{VIII} could border on values of order 1% for any value of $\tan\beta$, and it could even reach 4% for sufficiently small or big values of $\tan\beta$ within the interval (58). This result is quite remarkable, since it is about 60% of the QCD corrections to the canonical decay.

- **Decay IX**: This is a very interesting three-body decay to deal with, though its analysis is technically quite demanding for it involves four Feynman amplitudes (see Fig. 8). In the Appendix at the end of the paper we present the full squared amplitude corresponding to this particular decay. The parameter space includes as many as nine parameters, namely

$$(\tan\beta, m_{H^+}, \mu, M, m_{\tilde{g}}, m_{\tilde{b}_{1,2}}, m_{\tilde{t}_1}, M^t_{LR})\,. \tag{84}$$

In this case, and due to the potentiality of this mode, we relax the assumption on the stop mixing angle being $\theta_t = \pi/4$ and introduce the lightest stop mass $m_{\tilde{t}_1}$ as a new input. Furthermore, we also abandon the restriction $M^b_{LR} = 0$ and the assumption of degenerate sbottom masses by making allowance for a free input value of the sbottom mass eigenvalues $m_{\tilde{b}_{1,2}}$ with the proviso that $\theta_b = \pi/4$. In contrast to the previous decays, we shall not impose conditions blocking the possibility that the intermediate two-body states in Fig.8 can be real two-body decays, except for the gluino mode $t \to \tilde{t}\,\tilde{g}$ which, if allowed, would be overwhelming in most of the parameter space. As for the remaining two-body modes, it turns out that the present three-body decay can be competitive with them in certain regions of parameter space.

The numerical analysis of decay IX confirms the expected fact that it can be relevant only if the two-body channel $H^+ \to \tilde{t}\,\bar{\tilde{b}}$ is kinematically forbidden, otherwise the Higgs decay width becomes too large and it has a dramatic suppression effect on the partial width of our three-body decay. This can be seen in Fig.16a, corresponding to $m_{\tilde{t}} = 60$ GeV, $m_{\tilde{b}} = 100$ GeV, $m_{\tilde{g}} = 130$ GeV and a large value of $\tan\beta$ of order $m_t/m_b \simeq 36$. We have also fixed $\mu = M = 100, 250$ GeV and $M^b_{LR} = 0$. We see indeed that, for m_{H^+} approaching $m_{\tilde{t}} + m_{\tilde{b}}$ from below, the decay IX can give a contribution to the ratio

$$\delta_{IX} = \frac{\Gamma(t \to b\,\tilde{t}_1\,\bar{\tilde{b}}_1)}{\Gamma_{SM}}\,, \tag{85}$$

which ranges from a few percent to 100% and above. The contribution from $\tilde{b}_2$ is basically the same. Clearly, this behaviour is unmatched so far by any of the previous decays. Therefore, these non-standard effects are to be seriously considered in any

consistent treatment of the total top quark width. We postpone for Section 5 the discussion of the possible signatures.

Since in the conditions under study, the two-body mode $t \to H^+ b$ is still available, we also plot in Fig.16a the ratio

$$\frac{\Gamma(t \to H^+ b)}{\Gamma_{SM}} \,. \tag{86}$$

In this way we see that, depending on the value of μ, there may be a sizeable range of Higgs masses where the decay IX is not negligible as compared to the decay $t \to H^+ b$. Although these results have been obtained by assuming that the two sbottoms are degenerate, we may also use the general set of inputs (84) to enter different values for the sbottom masses. For example, take $m_{\tilde{b}_1} = 100$ GeV and $m_{\tilde{b}_2} = 150$ GeV, and set $\mu = 100$ GeV without altering the rest; we then obtain a rate $\delta_{IX} = 33\%$. In all these cases the soft SUSY-breaking parameter A_b is necessarily large to avoid conflict with the phenomenological mass bounds. In fact, if in the previous example we would trade the input parameter μ for A_b, we would find that we cannot demand a small input value $A_b \simeq 0$ since it would entail a too small a value of μ below 50 GeV, which is ruled out by the chargino mass bound (10).

Since the general set (84) is found not to change the order of magnitude of the rate of our decay, it will simplify the analysis to restore the original set of inputs

$$(\tan\beta, m_{H^+}, \mu, M, m_{\tilde{g}}, m_{\tilde{b}}, M^t_{LR}) \,. \tag{87}$$

where $\theta_t = \pi/4$, $M^b_{LR} = 0$ together with the assumption of degenerate sbottom masses. In Figs.16b and 16c we study the evolution of δ_{IX} versus $\tan\beta$ for the two regimes where the Higgs decay $H^+ \to \tilde{t}\,\bar{\tilde{b}}$ is closed and open, respectively. In the closed case the slope is very high in the large $\tan\beta$ region. As a consequence, the yield from the Higgs mediated diagram becomes so overwhelming at large $\tan\beta$ that the rate of the decay IX overtakes that of the canonical decay as soon as $\tan\beta \gtrsim 50$,!. Notice that the long flat region in the intermediate interval $1 \lesssim \tan\beta \lesssim 20$ is sustained by the gluino mediated diagram in Fig.8, though in this plateau the contribution stays small due to the large mass assumed for the gluino, which prevents the $t \to \tilde{t}\,\tilde{g}$ decay from occurring. Whereas the dependence on the soft SUSY-breaking parameter M is very mild, in Fig. 16d we exhibit the dramatic dependence on the parameter μ for typical values of the other parameters. As already mentioned, the region $\mu \lesssim 60$ GeV (which is unfavoured by our decay) is excluded by the present bounds on chargino masses. Notice also that when the real

Higgs decay into $\tilde{t}\,\bar{\tilde{b}}$ is viable the ratio δ_{IX} lessens considerably, viz. down a few percent level and mostly at a few per mil or below.

Intriguingly enough, there are regions of parameter space where the decay IX can be competitive with the main two-body modes available. In Figs. 17a and 17b we plot the two-body decay rates

$$\frac{\Gamma(t \to \tilde{t}_1\, \chi^0_\alpha)}{\Gamma_{SM}}\,, \qquad \frac{\Gamma(t \to \tilde{b}_a \chi^+_1)}{\Gamma_{SM}}\,, \tag{88}$$

as a function of $\tan\beta$ for two values of μ and for fixed $M_{\chi^+_1} = 60$ GeV. For the squark masses we have taken $m_{\tilde{b}_a} = 100$ GeV, $m_{\tilde{t}_1} = 60$ GeV. In the first decay we have included separated plots for the first three neutralinos $\chi^0_1, \chi^0_2, \chi^0_3$, since they are also allowed by phase space. Although the last two are heavier than χ^0_1 they are worth including, the reason being that they are more higgsino-like and therefore have larger Yukawa couplings of the form (35) resulting in a competitive contribution. For the second decay in (88), the chargino χ^+_2 has not been included since it is too heavy. It is seen that the rates can be high for small $\tan\beta$, and in this region they are more efficient than δ_{IX}. However, for $\tan\beta > 30$, the three-body decay width δ_{IX} is not only competitive but it can even surpass the rate of the previous two-body decays, especially for large enough μ where the partial width of the former increases substantially whereas the two-body partial widths (88) decrease.

- **Decay X**: This decay is similar to the previous one. The Feynman diagrams are similar to those in Fig. 8 by just replacing $\tilde{t} \to \tilde{\nu}_\tau$ and $\tilde{b} \to \tilde{\tau}$ and forgetting about gluino and neutralino mediated amplitudes. The parameter space for this decay reads

$$(\tan\beta, m_{H^+}, \mu, M^\tau_{LR}, m_{\tilde{\nu}_\tau}). \tag{89}$$

An obvious restriction to be fulfilled is

$$m_{\tilde{\nu}} < m_t - m_b - m_{\tilde{\tau}}\,. \tag{90}$$

For simplicity we shall assume that the two $\tilde{\tau}$-sleptons are degenerate in mass and that $M^\tau_{LR} = 0$. As in the decay IX, we expect that the ratio

$$\delta_X = \frac{\Gamma(t \to b\tilde{\nu}_\tau \tilde{\tau}^+_1)}{\Gamma_{SM}}\,, \tag{91}$$

will be most sizeable if the two-body Higgs decays $H^+ \to \tilde{\nu}_\tau \tilde{\tau}^+$ and $H^+ \to \tilde{t}\,\bar{\tilde{b}}$ are kinematically forbidden. If this is so, for m_{H^+} approaching $m_{\tilde{\nu}_\tau} + m_{\tilde{\tau}}$ from below, the decay X can furnish a contribution to the ratio δ_X which ranges between the few

percent to the several ten percent, depending on the value of the other parameters, specially of $\tan\beta$ and μ. This is seen in Fig.18a, where the relevant inputs are

$$(\tan\beta, \mu, m_{\tilde{\nu}_\tau}) = (40, 100 \text{ GeV}, 50 \text{ GeV}). \tag{92}$$

Cases $\tilde{\tau}_1$ and $\tilde{\tau}_2$ are almost indistinguishable since $\tan\beta$ is high in Fig. 18a. In Figs.18b and 18c we plot the evolution of δ_X on $\tan\beta$ and on μ, respectively, for fixed values of the other parameters. Notice that on increasing $\tan\beta$ the Higgs coupling to stau and the corresponding sneutrino increases but at the same time the stau mass also increases. For $m_{\tilde{\nu}_\tau} = 50$ GeV, this mass saturates at a value of $m_{\tilde{\tau}} \simeq 92$ GeV for $\tan\beta \simeq 10$. Therefore, for larger values of $\tan\beta$, the ratio δ_X steadily grows and it can surpass 50% for $\tan\beta \gtrsim 55$. These results can still be improved substantially for higher values of $|\mu|$ (Cf. Fig.18c).

5. Discussion and conclusions

To summarize, we see that there are some three body decays of the top quark within the MSSM whose contribution can be a fraction of the standard width $\Gamma_{SM} = \Gamma(t \to W^+ b)$ of order or above 1%. The latter reference value is approximately the size of the conventional electroweak quantum corrections to Γ_{SM} [34]. For the sake of comparison, let us point out that the Higgs effects on $t \to W^+ b$ within the MSSM are about one order of magnitude smaller than our reference value, i.e. they are of order 0.1%[22]. Many of our three-body decays could give a contribution above this small number. In general, however, we find that only a few number of these three-body decays do contribute, within the same order of perturbation theory, as much as the full (electroweak plus QCD) quantum effects on $t \to W^+ b$ in the SM, which are of order -7% [34]. Nonetheless, if we consistently add up the yield from some of these decays, we are able to find regions of the parameter space where the resultant pay-off could counterbalance the one-loop quantum effects. This could be the case e.g. if we add the contributions from decays I and IV within the heavy gluino scenario, or decays I and VIII within the light gluino scenario. In either of these situations the one-loop corrections would appear as "missing effects" in a measurement of the total width of the top quark, Γ_t. This feature is remarkable, since it is compatible with an scenario in which all of the SUSY two-body decays of the top quark are blocked up. In such a case the leading SUSY signature in *inclusive* top physics could come from the combined effect of the available three-body decays.

Finally, there are two cases, viz. decay IX and decay X, which could be very important in certain regions of parameter space, specifically in a region where both $\tan\beta$ and $|\mu|$ are large enough, $\tan\beta \gtrsim m_t/m_b \simeq 36$ and $|\mu| > 100$ GeV, provided that the Higgs mass is below the $\tilde{\nu}_\tau \tilde{\tau}^+$ and $\tilde{t}\,\bar{\tilde{b}}$ thresholds. In this case, the last two decays could contribute to the

total top quark width a fraction which, if one does not stretch too much the values of the relevant parameters, it can still range between the few percent to the several ten percent. The large size of these contributions are the tree-level counterpart, within the same order of perturbation theory, of the large one-loop quantum effects on the two-body decay (8) [26, 28][6]. Therefore, decays IX and X could possibly be searched as exclusive decays since they may give rise to well defined and rather exotic signatures. These signatures have to be compared with the canonical signature

$$t \to bW^+ \to b(f\bar{f}')\,, \tag{93}$$

which consists either of 3 jets (one of them a b-jet) or a b-jet + a positively charged lepton (l^+)+ missing energy-momentum ($\not{p}$). In Table 1 we display the alternative decay signatures associated to decay IX. In all cases we have obviated an additional b-jet which is in common with the canonical signature. Therefore, what we show is the specific signature associated to the virtual decay $H^+ \to \tilde{t}\bar{\tilde{b}}$ [33]. In some of the signatures in Table 1 (cases (a)-(c)) we have admitted of the exotic possibility to having FCNC decays mediated by neutralinos [21]. These could enter the game if the chargino decay mode of the stop,

$$\tilde{t}_1 \to b\chi_1^+\,, \tag{94}$$

is kinematically forbidden. If this mode is allowed, it would be dominant and the main signatures would be (d)-(f) in Table 1. As for the sbottom decay, the charged mode $\bar{\tilde{b}} \to \bar{c}\chi_1^+$ is CKM-suppressed whereas $\bar{\tilde{b}} \to \bar{b}\chi_1^0$ is always available (if a light neutralino exists). Let us point out that if the former case applies it would lead to two final leptons with the same electric charge (see case (f)), which is definitely a non-canonical signature. In general, we should expect that the leading signatures in Table 1 are (a)-(b) or (d)-(e), depending on whether the channel (94) is closed or open, respectively.

As far as decay X is concerned, a similar discussion ensues. The main signatures are detailed in Table 2. It could well happen that the charged sneutrino decay

$$\tilde{\nu}_\tau \to \tau^-\chi_1^+\,, \tag{95}$$

is phase space obstructed, similarly to the previous case (94) for the stop. However, an important difference here is that the neutral decay

$$\tilde{\nu}_\tau \to \nu_\tau\chi_1^0\,, \tag{96}$$

is perfectly possible and most likely it is the leading decay mode of the sneutrino, if χ_1^0 is the lightest SUSY particle. Another difference with respect to decay IX is that whereas the

[6]Notice that some of the Yukawa couplings (35) and triple scalar couplings (49) can be comparable to the strong gauge coupling (47). Therefore, the tree-level corrections to decay IX can be of the same order as the SUSY-QCD [26] and electroweak SUSY corrections [28] to the two-body decay (8).

charged decay of the sbottom is CKM-suppressed, the charged $\tilde{\tau}$-decay $\tilde{\tau}^+ \to \bar{\nu}_\tau \chi_1^+$ is not. We conclude that the leading signatures are (a)-(c) in Table 2, where the characteristic trait is the proliferation of jets, lepton prongs and missing energy. However, if the charged decay mode (95) would be available, it could be rather interesting, for the corresponding signatures (d)-(f) in Table 2 show the distinctive presence of a τ-lepton with the "wrong" sign, i.e a τ^-, in contradistinction to the canonical decay (93) where one expects to find a τ^+. Notice that in the conditions under study the signatures on Tables 1 and 2 cannot come from the decay of a real H^+; in fact, although real charged Higgs bosons can be produced in these conditions, their leading decay would be $H^+ \to \tau^+ \nu_\tau$. With enough statistics, the latter signature would lead to a violation of lepton universality and it has a chance to be isolated in the future (Cf. Section 4); however, with an insufficient statistics it could easily be confused with a standard signature (93). Quite in contrast, the exotic signatures displayed in Tables 1 and 2 are highly non-standard and may play an important role in the top quark phenomenology beyond the SM, especially in the analysis of the single top-quark production processes [30], which are foreseen to play a decisive role in the near future at Tevatron and at the LHC.

Acknowledgements:
One of us (J.S.) thanks A. Heinson for providing useful information on top quark physics at the Tevatron. This work has been partially supported by CICYT under project No. AEN95-0882. The work of J.G. has also been financed by a grant of the Comissionat per a Universitats i Recerca, Generalitat de Catalunya.

Appendix A

In this appendix we write out the full analytical expression for the squared amplitude of one single decay, since the complete formulae for all the processes that have been analyzed is extremely lengthy. We have chosen the decay IX, which is one of the most relevant candidates in the list of SUSY three-body modes presented on eq.(19). Using the Lagrangian interactions and coupling matrices defined on eqs. (33)-(34), (47)-(49), (52)-(54), along with the well-known SUSY Higgs-fermion interactions [17], one computes the Lorentz invariant amplitudes $T_i \, (i = 1, ..., 4)$ of the decay $t \to b \, \tilde{t}_b \, \bar{\tilde{b}}_a$ $(a, b = 1, 2)$ in terms of the four-momenta specified in Fig. 8a. The total squared amplitude summed over all final spin, colour and sflavour indices and averaged over the initial states can be casted in the following way:

$$\sum \langle |T|^2 \rangle = \sum_i Q_{ii} + \sum_{i<j} \left(Q_{ij} + Q_{ij}^\dagger \right) \tag{A.1}$$

where

$$Q_{ij} = \sum \langle T_i T_j^\dagger \rangle \, . \tag{A.2}$$

The explicit structure of the various Q_{ij} is rather cumbersome. We first do the following definitions[7]:

$$\begin{array}{lcl}
\epsilon_W & = & M_W \Gamma_W \\
\epsilon_H & = & m_{H^+} \Gamma_{H^+} \\
G_{ab} & = & g_{cd}\, R^{(b)}_{da}\, R^{(t)}_{cb} = g_{LL}\, R^{(b)}_{1a}\, R^{(t)}_{1b} + g_{RR}\, R^{(b)}_{2a}\, R^{(t)}_{2b} + g_{LR}\, R^{(b)}_{2a}\, R^{(t)}_{1b} + g_{RL}\, R^{(b)}_{1a}\, R^{(t)}_{2b} \\
Sum & = & \sum_{a,i,j,s,t} \lambda^a_{ij} \lambda^a_{st} = 12
\end{array}$$

and derive the following results:

$$\begin{array}{lcl}
Q_{aa} & = & \frac{3\, g^4\, {R^{(b)}_{1a}}^2\, {R^{(t)}_{1b}}^2}{4\left(\left({q_1}^2 - {m_W}^2\right)^2 + {\epsilon_W}^2\right)} \left(2\, \left(p_1 k - p_2 k\right)\, \left(p_1 p_3 - p_2 p_3\right) \right. \\
 & & - \left({m_{\tilde{b}}}^2 + {m_{\tilde{t}}}^2 - 2\, p_1 p_2\right)\, p_3 k \\
 & & - \frac{2\left({m_{\tilde{t}}}^2 - {m_{\tilde{b}}}^2\right)}{{m_W}^2}\, \left(k q_1\, \left(p_1 p_3 - p_2 p_3\right) - \left({m_{\tilde{t}}}^2 - {m_{\tilde{b}}}^2\right)\, p_3 k + \left(p_1 k - p_2 k\right)\, p_3 q_1\right) \\
 & & \left. + \frac{\left({m_{\tilde{t}}}^2 - {m_{\tilde{b}}}^2\right)^2}{{m_W}^4}\, \left(2\, k q_1\, p_3 q_1 - p_3 k\, {q_1}^2\right) \right)
\end{array}$$

$$\begin{array}{lcl}
Q_{bb} & = & \frac{3\, g^4\, {G_{ab}}^2}{4\, {m_W}^4 \left(\left({q_1}^2 - {m_{H^+}}^2\right)^2 + {\epsilon_{H^+}}^2\right)} \\
 & & \left(2\, {m_b}^2\, {m_t}^2 + p_3 k\, \left({m_t}^2 \cot\beta^2 + {m_b}^2 \tan\beta^2\right)\right)
\end{array}$$

$$\begin{array}{lcl}
Q_{cc} & = & \frac{8\, {g_s}^4}{3\left({q_2}^2 - {m_{\tilde{g}}}^2\right)^2} \left(2\, m_b\, {m_{\tilde{g}}}^2\, m_t\, R^{(b)}_{1a}\, R^{(b)}_{2a}\, R^{(t)}_{1b}\, R^{(t)}_{2b} \right. \\
 & & + 2\, m_b\, m_t\, {q_2}^2\, R^{(b)}_{1a}\, R^{(b)}_{2a}\, R^{(t)}_{1b}\, R^{(t)}_{2b} \\
 & & - 2\, m_{\tilde{g}}\, m_t\, p_3 q_2\, \left({R^{(b)}_{1a}}^2\, R^{(t)}_{1b}\, R^{(t)}_{2b} + {R^{(b)}_{2a}}^2\, R^{(t)}_{1b}\, R^{(t)}_{2b} \right) \\
 & & + {m_{\tilde{g}}}^2\, p_3 k\, \left({R^{(b)}_{2a}}^2\, {R^{(t)}_{1b}}^2 + {R^{(b)}_{1a}}^2\, {R^{(t)}_{2b}}^2 \right) \\
 & & - 2\, k q_2\, m_b\, m_{\tilde{g}}\, \left(R^{(b)}_{1a}\, R^{(b)}_{2a}\, {R^{(t)}_{1b}}^2 + R^{(b)}_{1a}\, R^{(b)}_{2a}\, {R^{(t)}_{2b}}^2 \right) \\
 & & \left. + \left(2\, k q_2\, p_3 q_2 - p_3 k\, {q_2}^2\right)\, \left({R^{(b)}_{1a}}^2\, {R^{(t)}_{1b}}^2 + {R^{(b)}_{2a}}^2\, {R^{(t)}_{2b}}^2 \right) \right)
\end{array}$$

[7]Here, for convenience, we express our results in real, instead of complex, matrix notation following the rules stated in Section 3.

$$
\begin{aligned}
Q_{d_\alpha d_\beta} &= \frac{3\,g^4}{4\left({q_2}^2-{m_{\chi^0}}_\alpha{}^2\right)\left({q_2}^2-{m_{\chi^0}}_\beta{}^2\right)}\ \Big(\\
&\quad {q_2}^2\,m_b\,m_t\ \left(A_{+a\beta}^{(0)b}\,A_{+b\beta}^{(0)t}\,A_{-a\alpha}^{(0)b}\,A_{-b\alpha}^{(0)t}+A_{-a\beta}^{(0)b}\,A_{-b\beta}^{(0)t}\,A_{+a\alpha}^{(0)b}\,A_{+b\alpha}^{(0)t}\right) \\
&\quad +\left(2\,kq_2\,p_3q_2-p_3k\,{q_2}^2\right)\ \left(A_{+a\beta}^{(0)b}\,A_{+b\beta}^{(0)t}\,A_{+a\alpha}^{(0)b}\,A_{+b\alpha}^{(0)t}+A_{-a\beta}^{(0)b}\,A_{-b\beta}^{(0)t}\,A_{-a\alpha}^{(0)b}\,A_{-b\alpha}^{(0)t}\right) \\
&\quad +p_3q_2\,m_t\,m_{{\chi^0}_\alpha}\ \left(A_{+a\beta}^{(0)b}\,A_{+b\beta}^{(0)t}\,A_{+a\alpha}^{(0)b}\,A_{-b\alpha}^{(0)t}+A_{-a\beta}^{(0)b}\,A_{-b\beta}^{(0)t}\,A_{-a\alpha}^{(0)b}\,A_{+b\alpha}^{(0)t}\right) \\
&\quad +kq_2\,m_b\,m_{{\chi^0}_\alpha}\ \left(A_{+a\beta}^{(0)b}\,A_{+b\beta}^{(0)t}\,A_{-a\alpha}^{(0)b}\,A_{+b\alpha}^{(0)t}+A_{-a\beta}^{(0)b}\,A_{-b\beta}^{(0)t}\,A_{+a\alpha}^{(0)b}\,A_{-b\alpha}^{(0)t}\right) \\
&\quad +p_3q_2\,m_t\,m_{{\chi^0}_\beta}\ \left(A_{-a\beta}^{(0)b}\,A_{+b\beta}^{(0)t}\,A_{-a\alpha}^{(0)b}\,A_{-b\alpha}^{(0)t}+A_{+a\beta}^{(0)b}\,A_{-b\beta}^{(0)t}\,A_{+a\alpha}^{(0)b}\,A_{+b\alpha}^{(0)t}\right) \\
&\quad +kq_2\,m_b\,m_{{\chi^0}_\beta}\ \left(A_{-a\beta}^{(0)b}\,A_{+b\beta}^{(0)t}\,A_{+a\alpha}^{(0)b}\,A_{+b\alpha}^{(0)t}+A_{+a\beta}^{(0)b}\,A_{-b\beta}^{(0)t}\,A_{-a\alpha}^{(0)b}\,A_{-b\alpha}^{(0)t}\right) \\
&\quad +m_b\,m_t\,m_{{\chi^0}_\alpha}\,m_{{\chi^0}_\beta}\ \left(A_{-a\beta}^{(0)b}\,A_{+b\beta}^{(0)t}\,A_{+a\alpha}^{(0)b}\,A_{-b\alpha}^{(0)t}+A_{+a\beta}^{(0)b}\,A_{-b\beta}^{(0)t}\,A_{-a\alpha}^{(0)b}\,A_{+b\alpha}^{(0)t}\right) \\
&\quad +p_3k\,m_{{\chi^0}_\alpha}\,m_{{\chi^0}_\beta}\ \left(A_{-a\beta}^{(0)b}\,A_{+b\beta}^{(0)t}\,A_{-a\alpha}^{(0)b}\,A_{+b\alpha}^{(0)t}+A_{+a\beta}^{(0)b}\,A_{-b\beta}^{(0)t}\,A_{+a\alpha}^{(0)b}\,A_{-b\alpha}^{(0)t}\right)\Big)
\end{aligned}
$$

$$
\begin{aligned}
Q_{ab}+Q_{ab}^\dagger &= \frac{3\,g^4\left(2\left({q_1}^2-{m_{H^+}}^2\right)\left({q_1}^2-{m_W}^2\right)+2\,\epsilon_{H^+}\,\epsilon_W\right)R_{1a}^{(b)}\,R_{1b}^{(t)}\,G_{ab}}{4\,{m_W}^2\left(\left({q_1}^2-{m_{H^+}}^2\right)^2+{\epsilon_{H^+}}^2\right)\left(({q_1}^2-{m_W}^2)^2+{\epsilon_W}^2\right)} \\
&\quad \Big(\left({m_t}^2\cot\beta\ \left(p_2p_3-p_1p_3+\frac{{m_{\tilde t}}^2-{m_{\tilde b}}^2}{{m_W}^2}\,p_3q_1\right)\right. \\
&\quad \left.+{m_b}^2\,\tan\beta\ \left(p_2k-p_1k+\frac{{m_{\tilde t}}^2-{m_{\tilde b}}^2}{{m_W}^2}\,kq_1\right)\right)
\end{aligned}
$$

$$
\begin{aligned}
Q_{ac}+Q_{ac}^\dagger &= \frac{g^2\,{g_s}^2\left({q_1}^2-{m_W}^2\right)Sum\,R_{1a}^{(b)}\,R_{1b}^{(t)}}{6\left(({q_1}^2-{m_W}^2)^2+{\epsilon_W}^2\right)\left({q_2}^2-{m_{\tilde g}}^2\right)} \\
&\quad \Big(\Big(kq_2\ \left(p_2p_3-p_1p_3+\frac{{m_{\tilde t}}^2-{m_{\tilde b}}^2}{{m_W}^2}\,p_3q_1\right)+\left(p_2k-p_1k+\frac{{m_{\tilde t}}^2-{m_{\tilde b}}^2}{{m_W}^2}\,kq_1\right)\,p_3q_2 \\
&\quad -p_3k\ \left(p_2q_2-p_1q_2+\frac{{m_{\tilde t}}^2-{m_{\tilde b}}^2}{{m_W}^2}\,q_1q_2\right)\Big)\ R_{1a}^{(b)}\,R_{1b}^{(t)} \\
&\quad -m_b\,m_{\tilde g}\ \left(p_2k-p_1k+\frac{{m_{\tilde t}}^2-{m_{\tilde b}}^2}{{m_W}^2}\,kq_1\right)\ R_{2a}^{(b)}\,R_{1b}^{(t)} \\
&\quad -m_{\tilde g}\,m_t\ \left(p_2p_3-p_1p_3+\frac{{m_{\tilde t}}^2-{m_{\tilde b}}^2}{{m_W}^2}\,p_3q_1\right)\ R_{1a}^{(b)}\,R_{2b}^{(t)} \\
&\quad +m_b\,m_t\ \left(p_2q_2-p_1q_2+\frac{{m_{\tilde t}}^2-{m_{\tilde b}}^2}{{m_W}^2}\,q_1q_2\right)\ R_{2a}^{(b)}\,R_{2b}^{(t)}\Big)
\end{aligned}
$$

$$
\begin{aligned}
Q_{ad}+Q_{ad}^\dagger &= \frac{3\,g^4\left({q_1}^2-{m_W}^2\right)R_{1a}^{(b)}\,R_{1b}^{(t)}}{2\left(({q_1}^2-{m_W}^2)^2+{\epsilon_W}^2\right)\left({q_2}^2-{m_{\chi^0}}_\alpha{}^2\right)}\ \Big(\\
&\quad \Big(kq_2\ \left(p_2p_3-p_1p_3+\frac{{m_{\tilde t}}^2-{m_{\tilde b}}^2}{{m_W}^2}\,p_3q_1\right)+\left(\frac{{m_{\tilde t}}^2-{m_{\tilde b}}^2}{{m_W}^2}\,kq_1-p_1k+p_2k\right)\,p_3q_2 \\
&\quad -p_3k\ \left(p_2q_2-p_1q_2+\frac{{m_{\tilde t}}^2-{m_{\tilde b}}^2}{{m_W}^2}\,q_1q_2\right)\Big)\ A_{+a\alpha}^{(0)b}\,A_{+b\alpha}^{(0)t} \\
&\quad +m_b\,m_t\ \left(p_2q_2-p_1q_2+\frac{{m_{\tilde t}}^2-{m_{\tilde b}}^2}{{m_W}^2}\,q_1q_2\right)\ A_{-a\alpha}^{(0)b}\,A_{-b\alpha}^{(0)t} \\
&\quad +m_b\,m_{{\chi^0}_\alpha}\ \left(p_2k-p_1k+\frac{{m_{\tilde t}}^2-{m_{\tilde b}}^2}{{m_W}^2}\,kq_1\right)\ A_{-a\alpha}^{(0)b}\,A_{+b\alpha}^{(0)t} \\
&\quad +m_t\,m_{{\chi^0}_\alpha}\ \left(-p_1p_3+p_2p_3+\frac{{m_{\tilde t}}^2-{m_{\tilde b}}^2}{{m_W}^2}\,p_3q_1\right)\ A_{+a\alpha}^{(0)b}\,A_{-b\alpha}^{(0)t}\Big)
\end{aligned}
$$

$$
\begin{aligned}
Q_{bc} + Q_{bc}^{\dagger} \;=\; & \frac{g^2\, {g_s}^2 \left({q_1}^2 - {m_{H^+}}^2\right) Sum\, G_{ab}}{6\, {m_W}^2 \left(\left({q_1}^2 - {m_{H^+}}^2\right)^2 + {\epsilon_{H^+}}^2\right)\left({q_2}^2 - {m_{\tilde{g}}}^2\right)} \Big(\\
& m_{\tilde{g}}\, p_3 k \, \left(-m_b \tan\beta\, R_{2a}^{(b)}\, R_{1b}^{(t)} - m_t \cot\beta\, R_{1a}^{(b)}\, R_{2b}^{(t)}\right) \\
& + m_b\, m_{\tilde{g}}\, m_t \, \left(-m_t \cot\beta\, R_{2a}^{(b)}\, R_{1b}^{(t)} - m_b \tan\beta\, R_{1a}^{(b)}\, R_{2b}^{(t)}\right) \\
& + m_b\, k q_2 \, \left(m_b \tan\beta\, R_{1a}^{(b)}\, R_{1b}^{(t)} + m_t \cot\beta\, R_{2a}^{(b)}\, R_{2b}^{(t)}\right) \\
& + m_t\, p_3 q_2 \, \left(m_t \cot\beta\, R_{1a}^{(b)}\, R_{1b}^{(t)} + m_b \tan\beta\, R_{2a}^{(b)}\, R_{2b}^{(t)}\right)\Big)
\end{aligned}
$$

$$
\begin{aligned}
Q_{bd} + Q_{bd}^{\dagger} \;=\; & \frac{3\, g^4 \left({q_1}^2 - {m_{H^+}}^2\right) G_{ab}}{2\, {m_W}^2 \left(\left({q_1}^2 - {m_{H^+}}^2\right)^2 + {\epsilon_{H^+}}^2\right)\left({q_2}^2 - {m_{\chi^0{}_\alpha}}^2\right)} \Big(\\
& m_b\, k q_2 \, \left(m_b \tan\beta\, A_{+a\alpha}^{(0)b}\, A_{+b\alpha}^{(0)t} + m_t \cot\beta\, A_{-a\alpha}^{(0)b}\, A_{-b\alpha}^{(0)t}\right) \\
& + m_t\, p_3 q_2 \, \left(m_t \cot\beta\, A_{+a\alpha}^{(0)b}\, A_{+b\alpha}^{(0)t} + m_b \tan\beta\, A_{-a\alpha}^{(0)b}\, A_{-b\alpha}^{(0)t}\right) \\
& + m_{\chi^0{}_\alpha}\, p_3 k \, \left(m_b \tan\beta\, A_{-a\alpha}^{(0)b}\, A_{+b\alpha}^{(0)t} + m_t \cot\beta\, A_{+a\alpha}^{(0)b}\, A_{-b\alpha}^{(0)t}\right) \\
& + m_b\, m_t\, m_{\chi^0{}_\alpha} \, \left(m_t \cot\beta\, A_{-a\alpha}^{(0)b}\, A_{+b\alpha}^{(0)t} + m_b \tan\beta\, A_{+a\alpha}^{(0)b}\, A_{-b\alpha}^{(0)t}\right)\Big)
\end{aligned}
$$

$$
\begin{aligned}
Q_{cd} \;=\; & \frac{g^2\, {g_s}^2\, Sum}{12 \left({q_2}^2 - {m_{\tilde{g}}}^2\right)\left({q_2}^2 - {m_{\chi^0{}_\beta}}^2\right)} \Big(\\
& - m_{\tilde{g}}\, m_t\, p_3 q_2 \, \left(A_{-a\beta}^{(0)b}\, A_{-b\beta}^{(0)t}\, R_{2a}^{(b)}\, R_{1b}^{(t)} + A_{+a\beta}^{(0)b}\, A_{+b\beta}^{(0)t}\, R_{1a}^{(b)}\, R_{2b}^{(t)}\right) \\
& - m_b\, m_{\tilde{g}}\, m_t\, m_{\chi^0{}_\beta} \, \left(A_{+a\beta}^{(0)b}\, A_{-b\beta}^{(0)t}\, R_{2a}^{(b)}\, R_{1b}^{(t)} + A_{-a\beta}^{(0)b}\, A_{+b\beta}^{(0)t}\, R_{1a}^{(b)}\, R_{2b}^{(t)}\right) \\
& - m_{\tilde{g}}\, m_{\chi^0{}_\beta}\, p_3 k \, \left(A_{-a\beta}^{(0)b}\, A_{+b\beta}^{(0)t}\, R_{2a}^{(b)}\, R_{1b}^{(t)} + A_{+a\beta}^{(0)b}\, A_{-b\beta}^{(0)t}\, R_{1a}^{(b)}\, R_{2b}^{(t)}\right) \\
& - m_b\, m_{\tilde{g}}\, k q_2 \, \left(A_{+a\beta}^{(0)b}\, A_{+b\beta}^{(0)t}\, R_{2a}^{(b)}\, R_{1b}^{(t)} + A_{-a\beta}^{(0)b}\, A_{-b\beta}^{(0)t}\, R_{1a}^{(b)}\, R_{2b}^{(t)}\right) \\
& + m_b\, m_t\, {q_2}^2 \, \left(A_{-a\beta}^{(0)b}\, A_{-b\beta}^{(0)t}\, R_{1a}^{(b)}\, R_{1b}^{(t)} + A_{+a\beta}^{(0)b}\, A_{+b\beta}^{(0)t}\, R_{2a}^{(b)}\, R_{2b}^{(t)}\right) \\
& + m_t\, , m_{\chi^0{}_\beta}\, p_3 q_2 \, \left(A_{+a\beta}^{(0)b}\, A_{-b\beta}^{(0)t}\, R_{1a}^{(b)}\, R_{1b}^{(t)} + A_{-a\beta}^{(0)b}\, A_{+b\beta}^{(0)t}\, R_{2a}^{(b)}\, R_{2b}^{(t)}\right) \\
& + m_b\, m_{\chi^0{}_\beta}\, k q_2 \, \left(A_{-a\beta}^{(0)b}\, A_{+b\beta}^{(0)t}\, R_{1a}^{(b)}\, R_{1b}^{(t)} + A_{+a\beta}^{(0)b}\, A_{-b\beta}^{(0)t}\, R_{2a}^{(b)}\, R_{2b}^{(t)}\right) \\
& + \left(2\, k q_2\, p_3 q_2 - p_3 k\, {q_2}^2\right) \, \left(A_{+a\beta}^{(0)b}\, A_{+b\beta}^{(0)t}\, R_{1a}^{(b)}\, R_{1b}^{(t)} + A_{-a\beta}^{(0)b}\, A_{-b\beta}^{(0)t}\, R_{2a}^{(b)}\, R_{2b}^{(t)}\right)\Big)
\end{aligned}
$$

The decay rate is obtained from the formulae above by converting all scalar products $p_i p_j \equiv p_i.p_j$ involved in these equations in terms of Mandelstam invariants S_1, S_2, S_3 and then by performing integration over them in the standard manner [48]. Care has to be exercised in the numerical integrations near the poles.

References

[1] F. Abe *et al.* (CDF Collab.), *Phys. Rev. Lett.* **74** (1995) 2626; S. Abachi *et al.* (D0 Collab.), *Phys. Rev. Lett.* **74** (1995) 2632.

[2] W. Bernreuther et al., Proc. of the Workshop on e^+e^- Collisions at 500 GeV: The Physics Potential, Hamburg, 1991, ed. P.M. Zerwas.

[3] C.-P. Yuan, *Top Quark Physics*, preprint-MSUHEP-50228 [hep-ph/9503216].

[4] For a recent status review, see e.g. W. Hollik, *Tests of the Standard Model*, Talk given at the International Europhysics Conference on High Energy Physics (HEP 95), Brussels, Belgium, 27 Jul - 2 Aug 1995 [hep-ph/9512232].

[5] D. Shaile, P.M. Zerwas, *Phys. Rev.* **D 45** (1992) 3262.

[6] P. Antilogus, *et al.,* (LEP Electroweak Working Group), preprint LEPEWWG/95-02, August 1995.

[7] M. Hildreth, talk given at the XXXIst Rencontres de Moriond on Electroweak Interactions and Grand Unified Theories, Les Arcs, March 1996, to appear in the Proceedings (eds. Frontières).

[8] H. Nilles, *Phys. Rep.* **110** (1984) 1; H. Haber and G. Kane, *Phys. Rep.* **117** (1985) 75; A. Lahanas and D. Nanopoulos, *Phys. Rep.* **145** (1987) 1; See also the exhaustive reprint collection *Supersymmetry* (2 vols.), ed. S. Ferrara (North Holland/World Scientific, Singapore, 1987); H.E. Haber, *Low-energy supersymmetry: prospects and challenges*, Invited talk at the International Workshop on Elementary Particle Physics, Present and Future, Valencia, Spain, June 1995, preprint CERN-TH/95-249 [hep-ph/9510412].

[9] M. Boulware, D. Finnell, *Phys. Rev.* **D 44** (1991) 2054; A. Djouadi, G. Girardi, C. Verzegnassi, W. Hollik, F.M. Renard, *Nucl. Phys.* **B 349** (1991) 48; G. Altarelli, R. Barbieri, F. Caravaglios, *Phys. Lett.* **B 314** (1993) 357; *Nucl. Phys.* **B 405** (1993) 3.

[10] J.D. Wells, C. Kolda, G.L. Kane, *Phys. Lett.* **B 338** (1994) 219; G.L. Kane, R.G. Stuart, J.D. Wells, *Phys. Lett.* **B 354** (1995) 350; P.H. Chankowski, S. Pokorski, preprint MPI-Ph/95-49 [hep-ph/9505308]; A. Dabelstein, W. Hollik, W. Mösle, preprint KA-THEP-5-1995 [hep-ph/9506251]; J.E. Kim, G.T. Park, *Phys.Rev.* **D 50** (1994) 6686; X. Wang, J.L. Lopez, D.V. Nanopoulos, preprint CERN-TH.7553/95 [hep-ph/9501258]; preprint CTP-TAMU-25/95 [hep-ph/9506217].

[11] D. Garcia, R.A. Jiménez, J. Solà, *Phys. Lett.* **B 347** (1995) 321 [E: **B 351** (1995) 602].

[12] D. Garcia, J. Solà, *Phys. Lett.* **B 354** (1995) 335.

[13] D. Garcia, J. Solà, *Phys. Lett.* **B 357** (1995) 349.

[14] J. Ellis, J.L. Lopez, D.V. Nanopoulos, preprint CERN-TH/95-314 [hep-ph/9512288]; A. Brignole, F. Feruglio, F. Zwirner, preprint CERN-TH/95-340 [hep-ph/9601293; P. Chankowski, S. Pokorski, preprint IFT-96/6 [hep-ph/9603310].

[15] J. Solà, *The top-quark width in the light of Z-boson physics*, preprint UAB-FT-372 [hep-ph/9508339], talk given at the Workshop on Physics of the Top Quark, Iowa State University, Ames, Iowa, May 1995, to appear in the Proceedings (World Scientific).

[16] J. Solà, *MSSM and Z width: implications on top quark and Higgs physics*, talk given at the XXXIst Rencontres de Moriond on Electroweak Interactions and Grand Unified Theories, Les Arcs, March 1996, to appear in the Proceedings (eds. Frontières).

[17] J.F. Gunion, H.E. Haber, G.L. Kane, S. Dawson, *The Higgs Hunters's Guide* (Addison-Wesley, Menlo-Park, 1990).

[18] H. Baer, M. Drees, R. Godbole, J.F. Gunion, X. Tata, *Phys. Rev.* **D 44** (1991) 725.

[19] K. Hidaka, Y. Kizukuri, *Phys. Lett.* **B 278** (1992) 278.

[20] F.M. Borzumati, Proc. of the Workshop Munich, Annecy, Hamburg, November 1992 to April 1993, P.M. Zerwas (Ed.), preprint DESY 93-123C, December 1993; F.M. Borzumati, N. Polonski, preprint TUM-T31-87-95 [hep-ph/9602433]; J. Sender, preprint UH-511-843-96 [hep-ph/9602354].

[21] S. Mrenna, C.-P. Yuan, *Phys. Lett.* **B 367** (1996) 188; J. Ellis, S. Rudaz, , *Phys. Lett.* **B 128** (1983) 248; I.I. Bigi, S. Rudaz, *Phys. Lett.* **B 153** (1985) 335; K. Hikasa, M. Kobayashi, *Phys. Rev.* **D 36** (1987) 724.

[22] B. Grzadkowski and W. Hollik, Nucl. Phys. **B384** (1992) 101; A. Denner and A.H. Hoang, Nucl. Phys. **B397** (1993) 483.

[23] D. Garcia, W. Hollik, R.A. Jiménez, J. Solà, *Nucl. Phys.* **B 427** (1994) 53.

[24] J.M. Yang, C.S. Li, *Phys. Lett.* **B 320** (1994) 117.

[25] A. Dabelstein, W. Hollik, R.A. Jiménez, C. Jünger, J. Solà, *Nucl. Phys.* **B 456** (1995) 75.

[26] J. Guasch, R.A. Jiménez, J. Solà, *Phys. Lett.* **B 360** (1995) 47.

[27] C.S. Li, J.M. Yang, *Phys. Lett.* **B 315** (1993) 367; H. König, *Phys. Rev.* **D 50** (1994) 3310.

[28] J. A. Coarasa, D. Garcia, J. Guasch, R.A. Jiménez, J. Solà, preprint UAB-FT (in preparation).

[29] S. Willenbrock, *Top Quark Physics at Fermilab*, talk presented at the International Symposium on Particle Theory and Phenomenology, Iowa State University, May 1995 [hep-ph/9508212], and talk presented in the XXXIst Rencontres de Moriond on Electroweak Interactions and Grand Unified Theories, Les Arcs, March 1996, to appear in the Proceedings (eds. Frontières); C. Quigg, preprint Fermilab-CONF-95/139-T [hep-ph/9507257].

[30] A.P. Heinson, *Electroweak Top Quark Production at the Fermilab Tevatron*, Talk given at the Workshop on Physics of the Top Quark, Ames, Iowa, May 1995; A.P. Heinson, A.S. Belyaev, E.E. Boos, preprint UCR/95-17 [hep-ph/9509274]; C.-P. Yuan, *Physics of Single-Top Quark Production at Hadron Colliders*, Talk given at the Workshop on Physics of the Top Quark, Ames, Iowa, May 1995.

[31] R.A. Jiménez, J. Solà, *Supersymmetric QCD corrections to the top quark decay of a heavy charged Higgs boson* preprint UAB-FT-376 [hep-ph/9511292].

[32] J. A. Coarasa, R.A. Jiménez, J. Solà, *Strong effects on the hadronic widths of the neutral Higgs bosons of the MSSM*, preprint UAB-FT-377 [hep-ph/9511402].

[33] A. Bartl, H. Eberl, K. Hidaka, T. Kon, W. Majerotto, Y. Yamada, preprint UWThPh-1995-35 [hep-ph/9511385]; A. Bartl, K. Hidaka, Y. Kizukuri, T. Kon, W. Majerotto, *Phys. Lett.* **B 315** (1993) 360.

[34] M. Jezabek and J.H. Kühn, *Nucl. Phys.* **B314** (1989) 1; *ibid* **B320** (1989) 20; C.S. Li, R.J. Oakes and T.C. Yuan, Phys. Rev. **D43** (1991) 3759; G. Eilam, R.R. Mendel, R. Migneron and A. Soni, *Phys. Rev. Lett.* **66** (1991) 3105; A. Denner and T. Sack, *Z. Phys.* **C46** (1990) 653; *Nucl. Phys.* **B 358** (1991) 46; B.A. Irwin, B. Magnolis and H.D. Trottier, *Phys. Lett.* **B256** (1991) 533; T.C. Yuan and C.-P. Yuan, *Phys. Rev.* **D44** (1991) 3603.

[35] K. Fujii, T. Matsui, *Phys. Rev.* **50** (1994) 4341.

[36] G.F. Tartarelli, talk given at the XXXIst Rencontres de Moriond on Electroweak Interactions and Grand Unified Theories, Les Arcs, March 1996, to appear in the Proceedings (eds. Frontières).

[37] V. Fadin, V. Khoze, *Sov. J. Nucl. Phys.* **48** (1988) 309; M. Strassler, M. Peskin, *Phys. Rev.* **D 43** (1991) 1500.

[38] LEP Collaborations, *First results from the 130/136 LEP run*, CERN, Geneve, December 12th, 1995; talks by J. Nachtman and P. Rebecchi in the XXXIst Rencontres de Moriond on Electroweak Interactions and Grand Unified Theories, Les Arcs, March 1996, to appear in the Proceedings (eds. Frontières).

[39] J. Ellis, G. Ridolfi, F. Zwirner, *Phys. Lett.* **B 257** (1991) 54; **B 262** (1991) 477; A. Brignole, J. Ellis, G. Ridolfi, F. Zwirner, *Phys. Lett.* **B 271** (1991) 123; H.E. Haber, R. Hempfling, *Phys. Rev. Lett.* **66** (1991) 1815; *Phys. Rev.* **D 48** (1993) 4280.

[40] L. Clavelli, *Phys. Rev.* **D 46** (1992) 2112; L. Clavelli, P. Coulter, K. Yuan, *Phys. Rev.* **D 47** (1993) 1973; M. Jezabek, J.H. Kühn, *Phys. Lett.* **B 301** (1993) 121; J. Ellis, D.V. Nanopoulos, D.A. Ross, *Phys. Lett.* **B 305** (1993) 375.

[41] F. Abe et. al., (CDF Collab.), *Phys. Rev.* **69** (1992) 3439; A. Para (D0 Collab.), talk presented at the International Symposium on Particle Theory and Phenomenology, Ames, Iowa, May 1995 (To appear in the Proceedings).

[42] J.F. Gunion, H. Haber, *Nucl. Phys.* **B 272** (1986) 1.

[43] Review of Particle Properties, *Phys. Rev.* **D 50** (1994).

[44] J. Guasch, Diploma Thesis, Univ. Autònoma de Barcelona, January 1996.

[45] F. Abe *et al.* (CDF Collab.), *Phys. Rev. Lett.* **72** (1994) 1977.

[46] Atlas Collab., *Atlas technical proposal for a general-purpose pp experiment at the Large Hadron Collider at CERN*, preprint CERN/LHCC/94-43, December 1944, pp. 245-248.

[47] S. Raychaudhuri, D.P. Roy, preprint TIFR/TH/95-08 [hep-ph/9503251] and TIFR/TH/95-35 [hep-ph/9507388].

[48] E. Byckling, K. Kajantie, *Particle Kinematics* (John Wiley & Sons, 1973).

Figure Captions

- **Fig.1** Feynman diagrams for the decay **I**. Diagram **(a)** is the SM amplitude, and diagram **(b)** is the extra charged Higgs contribution in the MSSM.

- **Fig.2** Feynman diagrams for the decay **II**.

- **Fig.3** Feynman diagrams for the decay **III**.

- **Fig.4** Feynman diagrams for the decay **IV**.

- **Fig.5** Feynman diagrams for the decay **V**.

- **Fig.6** Feynman diagrams for the decays **VI (a)** and **VII (b)**.

- **Fig.7** Feynman diagrams for the decay **VIII**.

- **Fig.8** Feynman diagrams for the decay **IX**. Those for the decay **X** are obtained from **(a)** and **(b)** after replacing $\tilde{t} \to \tilde{\nu}_\tau$ and $\tilde{b} \to \tilde{\tau}$.

- **Fig. 9** Isolines of δ_I in the $\tan\beta$-m_{H^+} plane.

- **Fig. 10** δ_{II} as a function of $\tan\beta$ for two values of m_{H^+}.

- **Fig. 11** δ_{III} as a function of $m_{\tilde{b}}$ for a $\tilde{b}_L$ final state, with $\tan\beta = 1$ and $m_{\tilde{g}} = 1$ GeV.

- **Fig. 12** Maximum value of δ_{IV} as a function of $\tan\beta$, for $m_{\tilde{b}} = 125$ GeV, $m_{\tilde{t}} = 155$ GeV, $m_{H^+} = 175$ GeV and $m_{\chi_1^+} = 60$ GeV.

- **Fig. 13** Lattice plot sampling of δ_V for $\tilde{b}_L$ and $\tilde{b}_R$ final states as a function of $m_{\tilde{b}}$, with $\tan\beta = 40$, $m_{\tilde{g}} = 140$ GeV, $-5M_Z < \mu < 5M_Z$, $0 < M < 5M_Z$, and 125 GeV $< M^t_{LR} <$ 230 GeV. In this case we have used $m_{\chi_1^+} > 50$ GeV.

- **Fig. 14 (a)** Maximum value of δ_{VII} as a function of $\tan\beta$ for $m_{\chi_1^+} = 135$ GeV and $m_{\tilde{b}} = m_{\tilde{s}} = 50$ GeV; **(b)** As before, but for δ_{VIII} and $m_{\tilde{\tau}} = 95$ GeV.

- **Fig. 15** Maximum value of δ_{VIII} for fixed $m_{\tilde{g}} = 1$ GeV, $m_{\tilde{t}} = 190$ GeV and $m_{\tilde{b}} = 150$ GeV. The maximum is attained at points on the (μ, M)-plane corresponding to the phenomenological limit $m_{\chi_1^+} = 60$ GeV.

- **Fig. 16 (a)** δ_{IX} as a function of m_{H^+} for $\tan\beta = 36$, $m_{\tilde{t}} = 60$ GeV, $m_{\tilde{b}} = 100$ GeV, $m_{\tilde{g}} = 130$ GeV and $\mu = 100$ GeV, 250 GeV. Also plotted is the ratio $\Gamma(t \to bH^+)/\Gamma_{SM}$; **(b)** δ_{IX} versus $\tan\beta$ for $\mu = 100$ GeV and a charged Higgs mass value below the $\tilde{t}\bar{\tilde{b}}$ threshold; **(c)** As in (b) but for a charged Higgs mass above the $\tilde{t}\bar{\tilde{b}}$ threshold; **(d)** δ_{IX} as a function of μ, for the same inputs as in (b) and $\tan\beta = 36$.

- **Fig. 17 (a)** $\Gamma(t \to \tilde{t}\,\chi^0_\alpha)/\Gamma_{SM}$ for the first three lightest neutralinos as a function of $\tan\beta$ for $m_{\chi^+_1} = 60$ GeV, $m_{\tilde{t}} = 60$ GeV and $\mu = 100$ GeV, 250 GeV; **(b)** As before, but for the decay $t \to \tilde{b}_a\,\chi^+_1$ and $m_{\tilde{b}} = 100$ GeV.

- **Fig. 18 (a)** δ_X as a function of m_{H^+} for $\tan\beta = 36$, $m_{\tilde{\nu}} = 50$ GeV and $\mu = 100$ GeV; **(b)** δ_X versus $\tan\beta$ for $m_{H^+} = 140$ GeV; **(c)** δ_X as a function of μ for the same inputs as before.

Typical Decays	Signal
(a) $\begin{cases} \tilde{t}_1 \to c\chi^0_1 \\ \bar{\tilde{b}}_{1,2} \to \bar{b}\chi^0_1 \end{cases}$	2 j's + $\not{p}$ (more $\not{p}$, less b activity)
(b) $\begin{cases} \tilde{t}_1 \to c\chi^0_1 \\ \bar{\tilde{b}}_{1,2} \to \bar{b}\chi^0_2 \to \begin{bmatrix} \bar{b}(Z^{(*)})\chi^0_1 \to \bar{b}(f\bar{f})\chi^0_1 \\ \text{or} \\ \bar{b}(h^0\chi^0_1) \to \bar{b}(b\bar{b} \text{ or } \tau^+\tau^-)\chi^0_1 \end{bmatrix} \end{cases}$	4 j's + $\not{p}$; 2 j's + $\not{p}$; 2 j's + $l^+\,l^-$ + $\not{p}$. (Z^0 or h^0 emission; more b activity if h^0 or $Z^0 \to b\bar{b}$; less b activity if h^0 or $Z^0 \to f\bar{f}$ or $\nu\bar{\nu}$)
(c) $\begin{cases} \tilde{t}_1 \to c\chi^0_1 \\ \bar{\tilde{b}}_2 \to \bar{c}\chi^+_1 \to \bar{c}(f\bar{f}'\chi^0_1) \end{cases}$	4 j's + $\not{p}$; 2 j's + l^+ + $\not{p}$. (isolated lepton l^+)
(d) $\begin{cases} \tilde{t}_1 \to b\chi^+_1 \to b(f\bar{f}'\chi^0_1) \\ \bar{\tilde{b}}_{1,2} \to \bar{b}\,\chi^0_1 \end{cases}$	4 j's + $\not{p}$; 2 j's + l^+ + $\not{p}$. (more $\not{p}$, more b activity)
(e) $\begin{cases} \tilde{t}_1 \to b\chi^+_1 \to b(f\bar{f}'\chi^0_1) \\ \bar{\tilde{b}}_{1,2} \to \bar{b}\,\chi^0_2 \to \begin{bmatrix} \bar{b}(Z^{(*)})\chi^0_1) \to \bar{b}(f\bar{f})\chi^0_1 \\ \text{or} \\ \bar{b}(h^0\chi^0_1) \to \bar{b}(b\bar{b} \text{ or } \tau^+\tau^-)\chi^0_1 \end{bmatrix} \end{cases}$	6 j's + $\not{p}$; 4 j's + $l^+\,l^-$ + $\not{p}$; 4 j's + l^+ + $\not{p}$; 4 j's + $\not{p}$; 2 j's + $l^+l^-\,l'^+$ + $\not{p}$; 2 j's + l^+ + $\not{p}$. (Z^0 or h^0 emission; more b activity if h^0 or $Z^* \to b\bar{b}$; Trilepton)
(f) $\begin{cases} \tilde{t}_1 \to b\chi^+_1 \to b(f\bar{f}'\chi^0_1) \\ \bar{\tilde{b}}_{1,2} \to \bar{c}\chi^+_1 \to \bar{c}(f\bar{f}'\chi^0_1) \end{cases}$	6 j's + $\not{p}$; 4 j's + l^+ + $\not{p}$; 2 j's + $l^+\,l'^+$ + $\not{p}$. (dilepton of same sign)

Table 1: Detection signatures for the decay **IX**. The decay chains (a)-(c) are possible only if $m_{\tilde{t}_1} < m_{\chi^+_1,\tilde{l},\tilde{\nu},\tilde{b}}$ and $m_{\chi^0_1} < m_{\tilde{t}_1}$. The decay chains (d)-(f) are possible only if $m_{\tilde{t}_1} > m_{\chi^+_1}$. Here $\not{p}$,j,$l^\pm$,$Z^{(*)}$ and f denote missing energy-momentum, jet, isolated charged lepton, Z^0 real or virtual, and $(q, l^\pm, \nu)$, respectively.

Typical Decays	Signal
(a) $\begin{cases} \tilde{\nu}_\tau \to \nu_\tau \chi_1^0 \\ \tilde{\tau}_{1,2}^+ \to \tau^+ \chi_1^0 \end{cases}$	$\tau^+ + \not{p}$ (more $\not{p}$)
(b) $\begin{cases} \tilde{\nu}_\tau \to \nu_\tau \chi_1^0 \\ \tilde{\tau}_{1,2}^+ \to \tau^+ \chi_2^0 \to \left[\begin{array}{l} \tau^+(Z^{(*)})\chi_1^0 \to \tau^+(f\bar{f})\chi_1^0 \\ \text{or} \\ \tau^+(h^0\chi_1^0) \to \tau^+(b\bar{b} \text{ or } \tau^+\tau^-)\chi_1^0 \end{array} \right. \end{cases}$	2 j's + $\tau^+ + \not{p}$; $\tau^+ + l^+ l^- + \not{p}$. ($Z^0$ or h^0 emission; more b activity if h^0 or $Z^0 \to b\bar{b}$; less b activity if h^0 or $Z^0 \to f\bar{f}$ or $\nu\bar{\nu}$)
(c) $\begin{cases} \tilde{\nu}_\tau \to \nu_\tau \chi_1^0 \\ \tilde{\tau}_{1,2}^+ \to \bar{\nu}_\tau \chi_1^+ \to \nu_\tau (f\bar{f}' \chi_1^0) \end{cases}$	2 j's + $\not{p}$; $l^+ + \not{p}$. (isolated lepton; less b activity)
(d) $\begin{cases} \tilde{\nu}_\tau \to \tau^- \chi_1^+ \to \tau^- (f\bar{f}' \chi_1^0) \\ \tilde{\tau}_{1,2}^+ \to \tau^+ \chi_1^0 \end{cases}$	2 j's + $\tau^+\tau^- + \not{p}$; $l^+ + \tau^+\tau^- + \not{p}$. (more $\not{p}$)
(e) $\begin{cases} \tilde{\nu}_\tau \to \tau^- \chi_1^+ \to \tau^- (f\bar{f}' \chi_1^0) \\ \tilde{\tau}_{1,2}^+ \to \tau^+ \chi_2^0 \to \left[\begin{array}{l} \tau^+(Z^{(*)})\chi_1^0 \to \tau^+(f\bar{f})\chi_1^0 \\ \text{or} \\ \tau^+(h^0\chi_1^0) \to \tau^+(b\bar{b} \text{ or } \tau^+\tau^-)\chi_1^0 \end{array} \right. \end{cases}$	4 j's + $\tau^+\tau^- + \not{p}$; 2 j's + $\tau^+\tau^- + l^+ l^- + \not{p}$; 2 j's + $\tau^+\tau^- + l^+ + \not{p}$; $\tau^+\tau^- + l^+ + l'^+ l'^- + \not{p}$. ($Z^0$ or h^0 emission; more b activity if h^0 or $Z^* \to b\bar{b}$; trilepton)
(f) $\begin{cases} \tilde{\nu}_\tau \to \tau^- \chi_1^+ \to \tau^- (f\bar{f}' \chi_1^0) \\ \tilde{\tau}_2^+ \to \bar{\nu}_\tau \chi_1^+ \to \bar{\nu}_\tau (f\bar{f}' \chi_1^0) \end{cases}$	4 j's + $\tau^- + \not{p}$; 2 j's + $\tau^- + l^+ + \not{p}$; $\tau^- + l^+ l'^+ + \not{p}$. ("wrong"-sign single τ lepton; same sign dilepton)

Table 2: Detection signatures for the decay **X**. The decay chains (a)-(c) are possible only if $m_{\tilde{\nu}} > m_{\chi_1^0}$. The decay chains (d)-(f) are possible only if $m_{\tilde{\nu}} > m_{\chi_1^+}$. Here $\not{p}$,j,$l^\pm$,$Z^{(*)}$ and f denote missing energy-momentum, jet, isolated charged lepton, Z^0 real or virtual, and $(q, l^\pm, \nu)$, respectively.

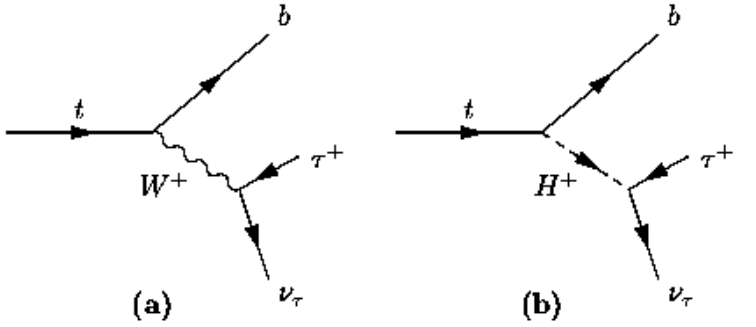

Fig. 1

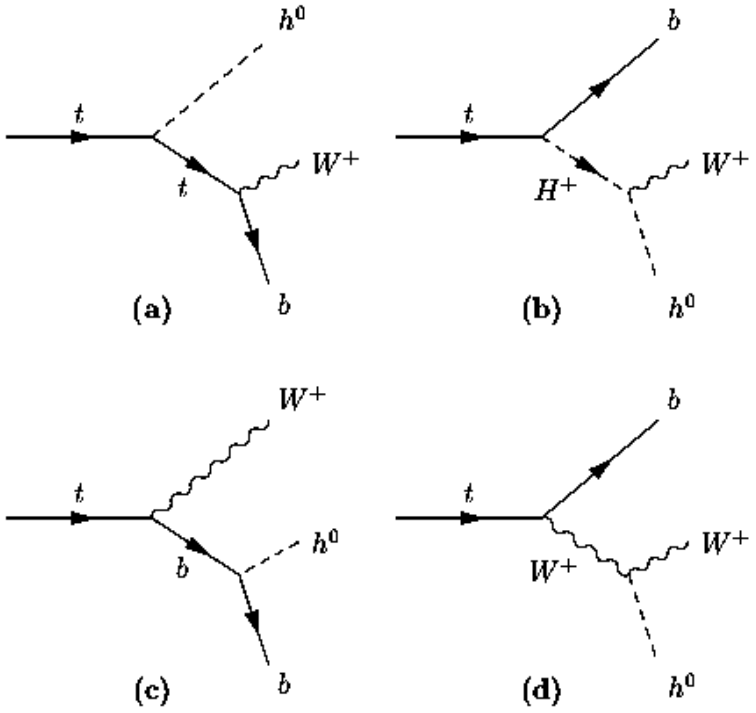

Fig. 2

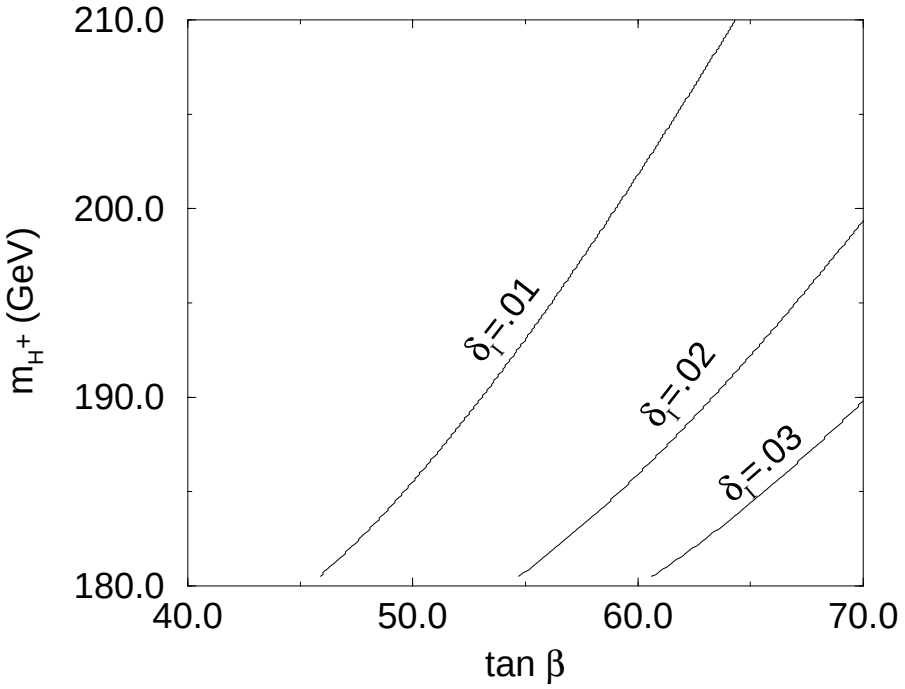
210.0
200.0
190.0
180.0
40.0
50.0
60.0
70.0
m_H+ (GeV)
tan β
δ_I=.01
δ_I=.02
δ_I=.03

Fig. 9

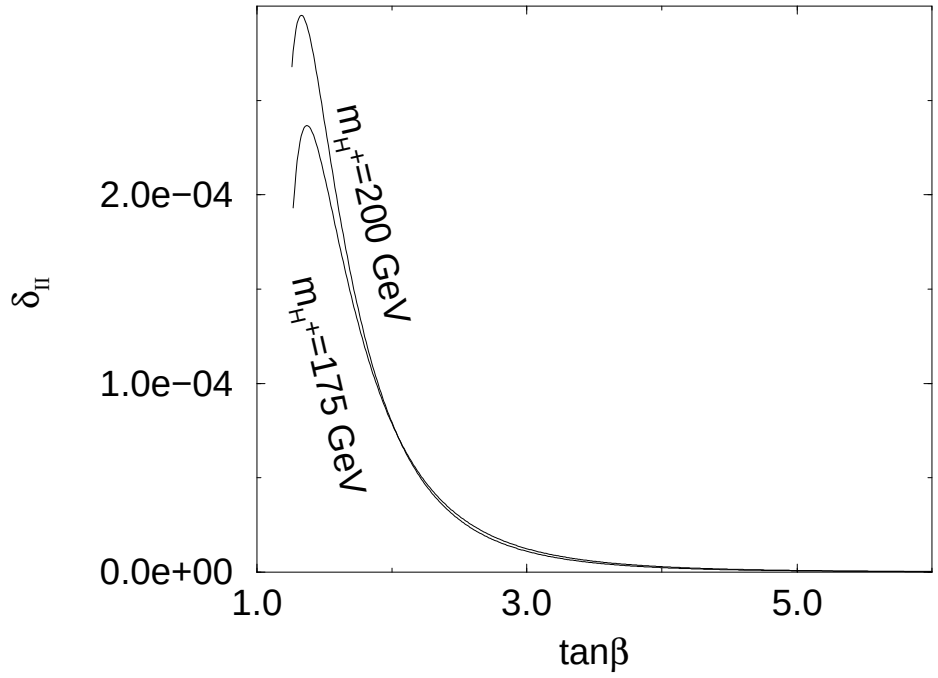
2.0e−04
1.0e−04
0.0e+00
1.0
3.0
5.0
δ_II
tanβ
m_H+=200 GeV
m_H+=175 GeV

Fig. 10

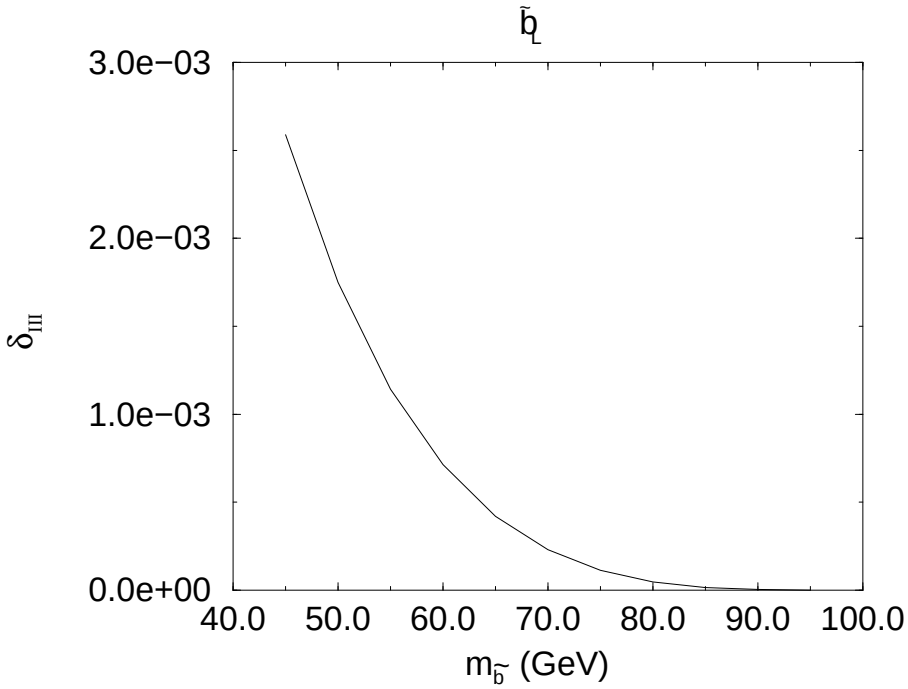
$\tilde{b}_L$
3.0e−03
2.0e−03
1.0e−03
0.0e+00
δ_{III}
40.0
50.0
60.0
70.0
80.0
90.0
100.0
$m_{\tilde{b}}$ (GeV)

Fig. 11

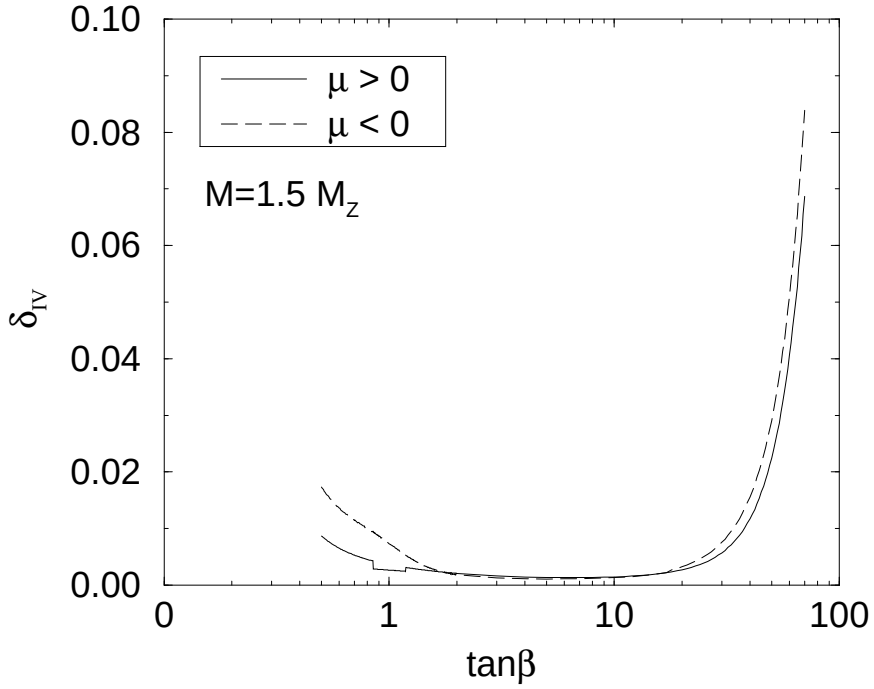
0.10
0.08
0.06
0.04
0.02
0.00
δ_{IV}
μ > 0
μ < 0
M=1.5 M_Z
0
1
10
100
tanβ

Fig. 12

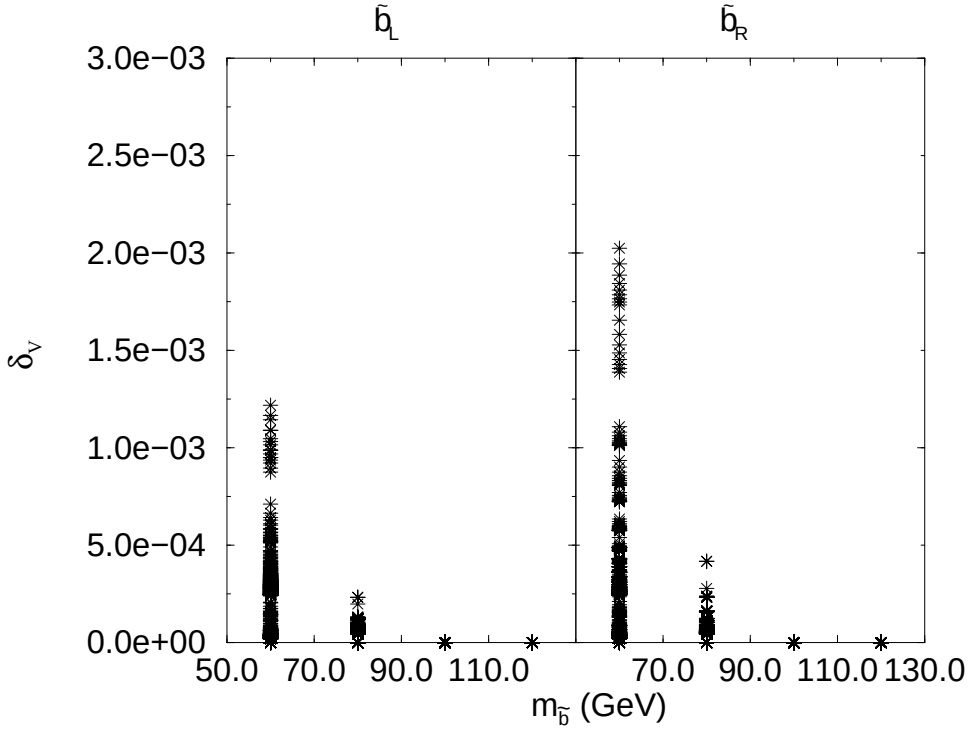

Fig. 13

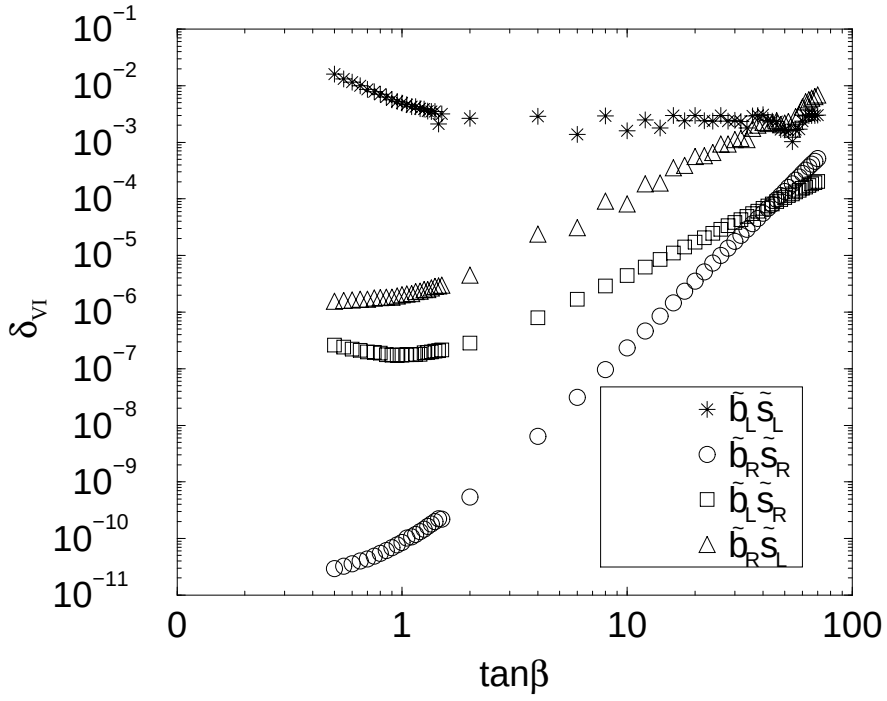

(a)

Fig. 14

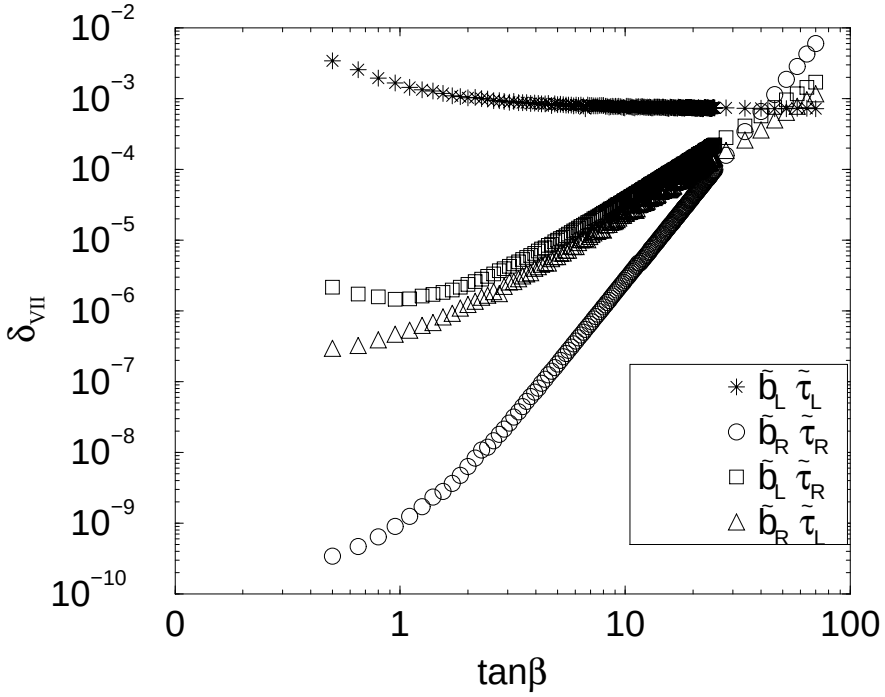

(b)

Fig. 14

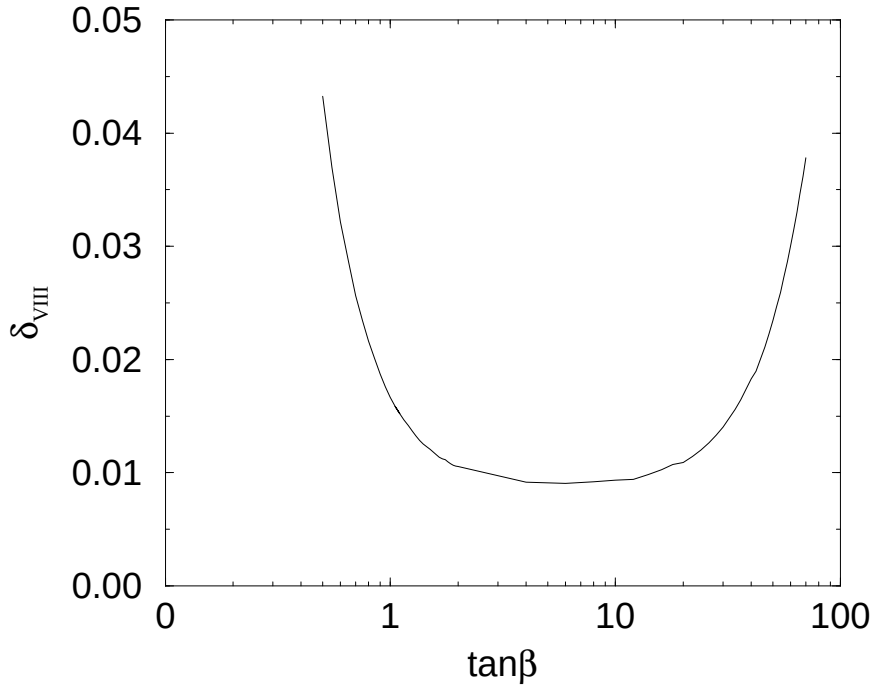

Fig. 15

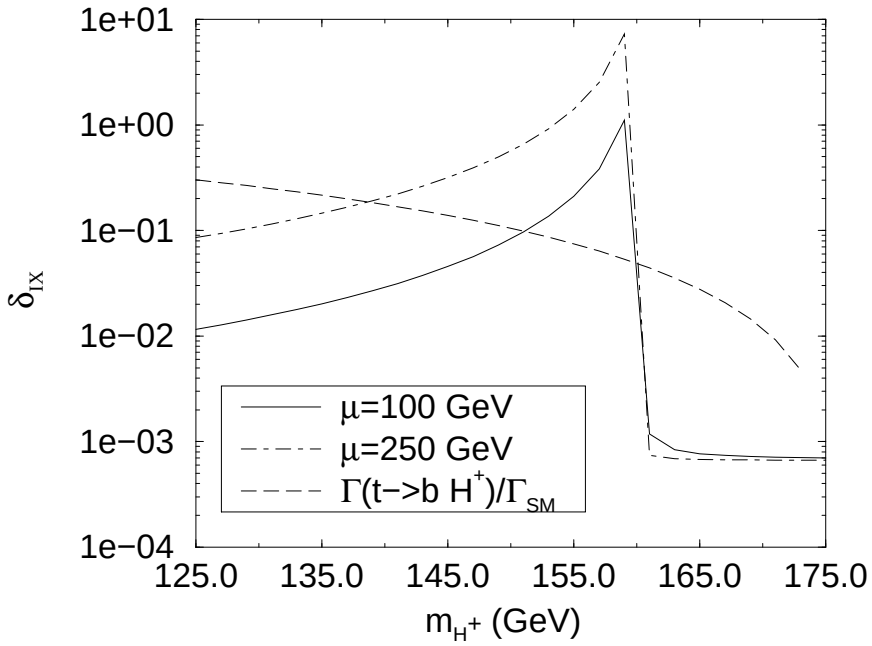
1e+01
1e+00
1e−01
1e−02
1e−03
1e−04
$\delta_{\Gamma X}$
μ=100 GeV
μ=250 GeV
$\Gamma(t->b\ H^+)/\Gamma_{SM}$
125.0
135.0
145.0
155.0
165.0
175.0
m_{H^+} (GeV)

(a)

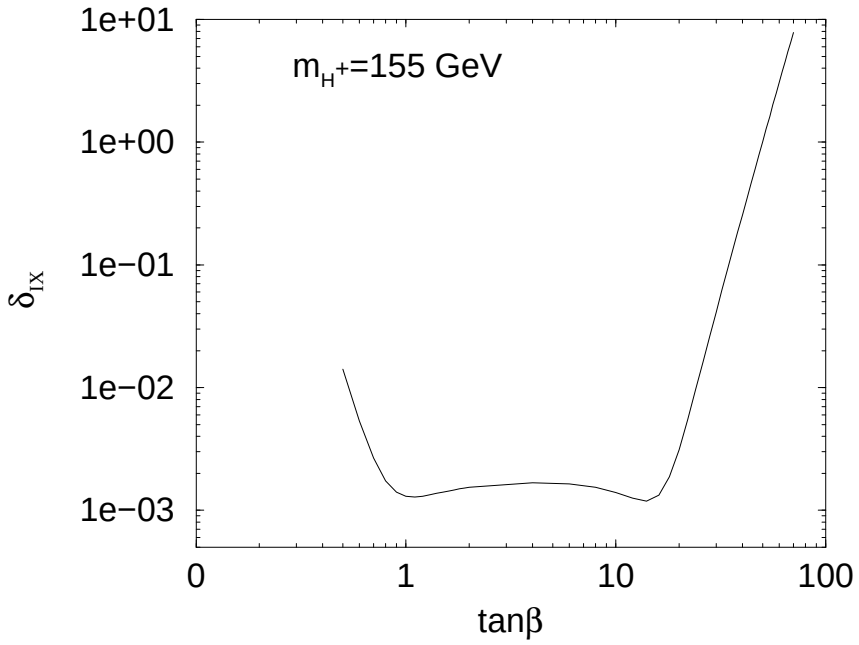
1e+01
1e+00
1e−01
1e−02
1e−03
$\delta_{\Gamma X}$
m_{H^+}=155 GeV
0
1
10
100
tanβ

(b)

Fig. 16

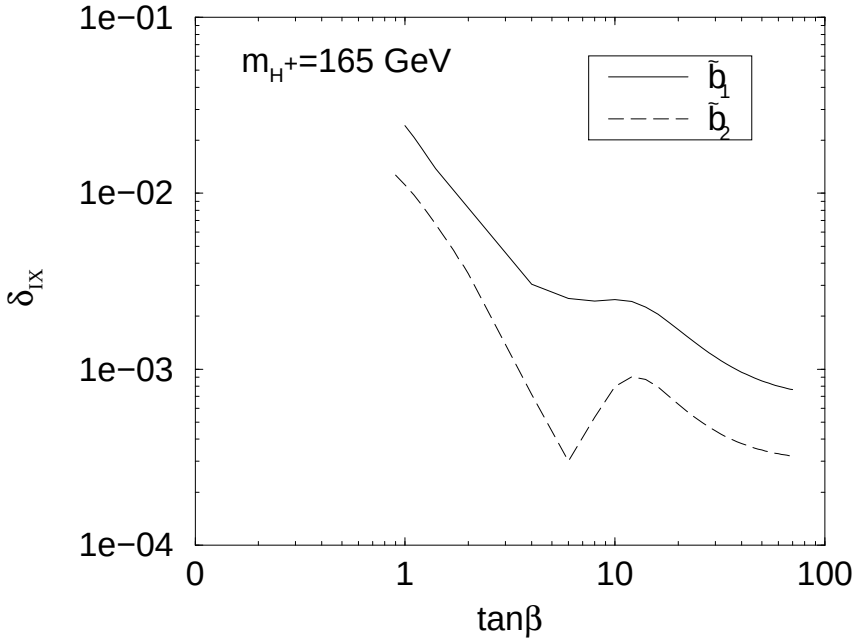
1e−01
1e−02
1e−03
1e−04
m_{H^+}=165 GeV
$\tilde{b}_1$
$\tilde{b}_2$
δ_{IX}
0
1
10
100
tanβ

(c)

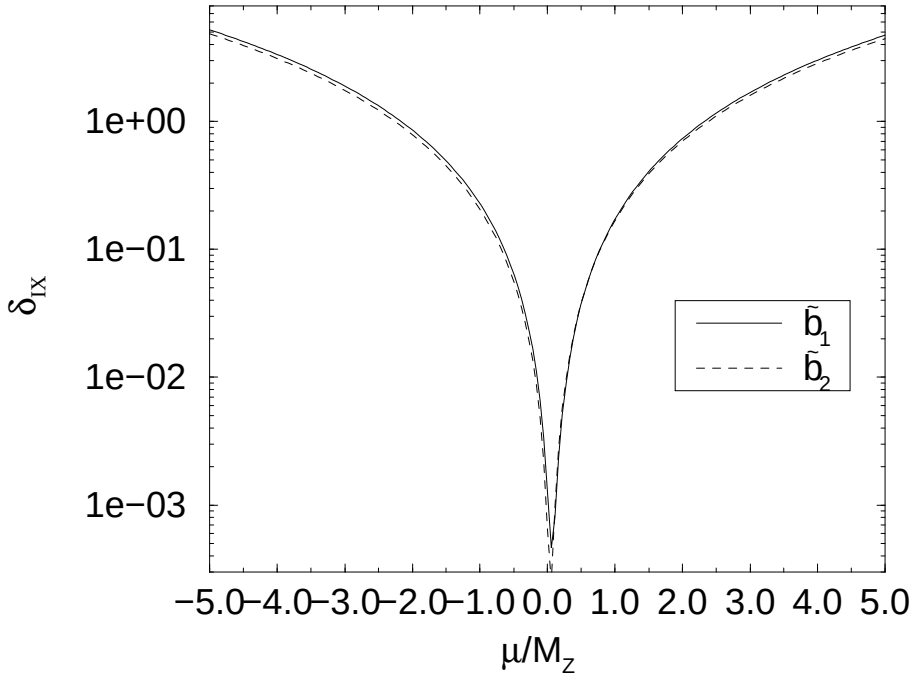
1e+00
1e−01
1e−02
1e−03
$\tilde{b}_1$
$\tilde{b}_2$
δ_{IX}
−5.0 −4.0 −3.0 −2.0 −1.0 0.0 1.0 2.0 3.0 4.0 5.0
μ/M_Z

(d)

Fig. 16

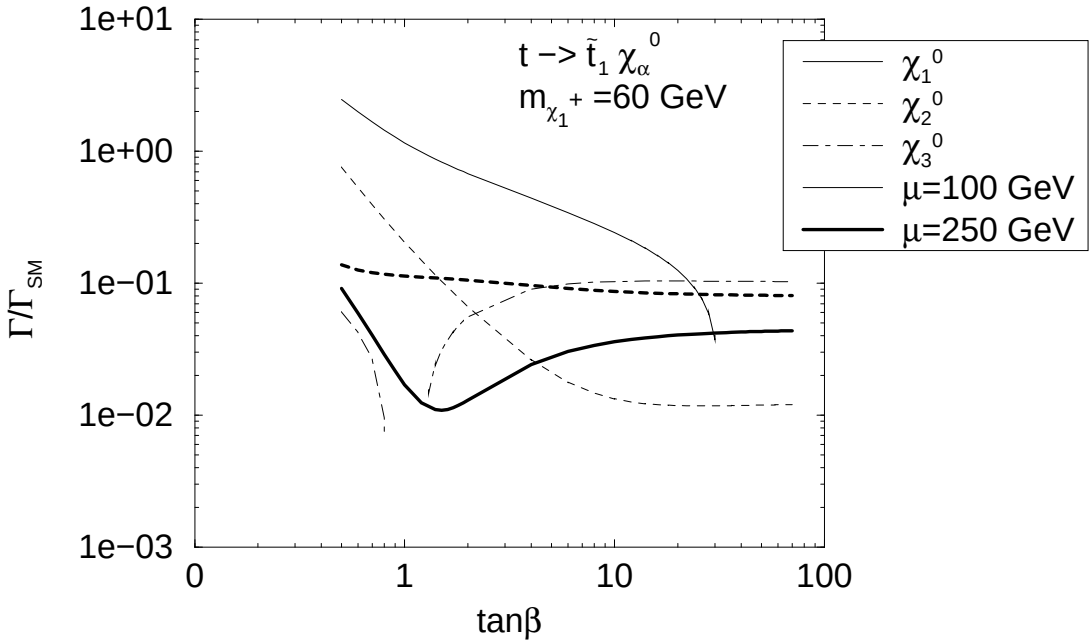
1e+01
1e+00
1e−01
1e−02
1e−03
0
1
10
100
tanβ
Γ/Γ_SM
t −> t̃_1 χ_α^0
m_χ1+ =60 GeV
χ_1^0
χ_2^0
χ_3^0
μ=100 GeV
μ=250 GeV

(a)

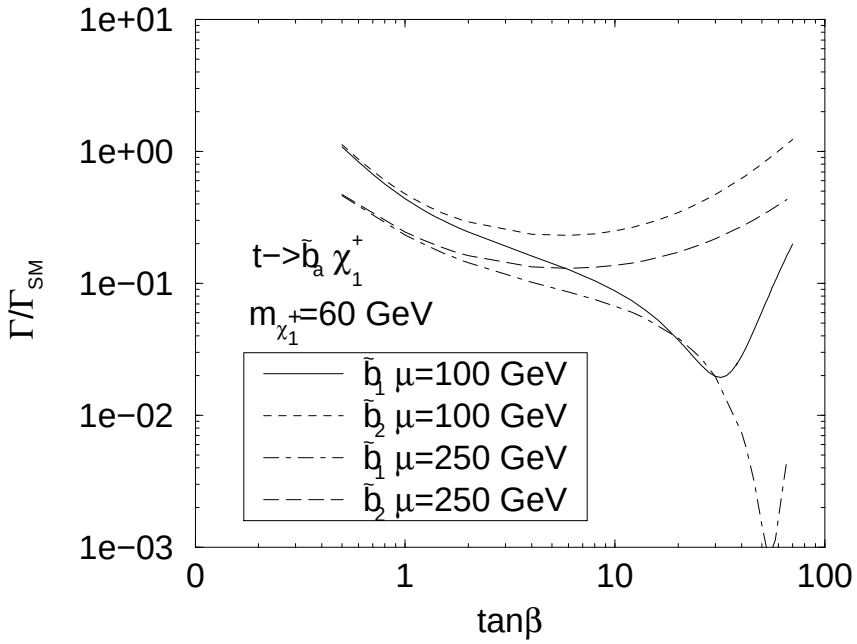
1e+01
1e+00
1e−01
1e−02
1e−03
0
1
10
100
tanβ
Γ/Γ_SM
t−>b̃_a χ_1^+
m_χ1+=60 GeV
b̃_1 μ=100 GeV
b̃_2 μ=100 GeV
b̃_1 μ=250 GeV
b̃_2 μ=250 GeV

(b)

Fig. 17

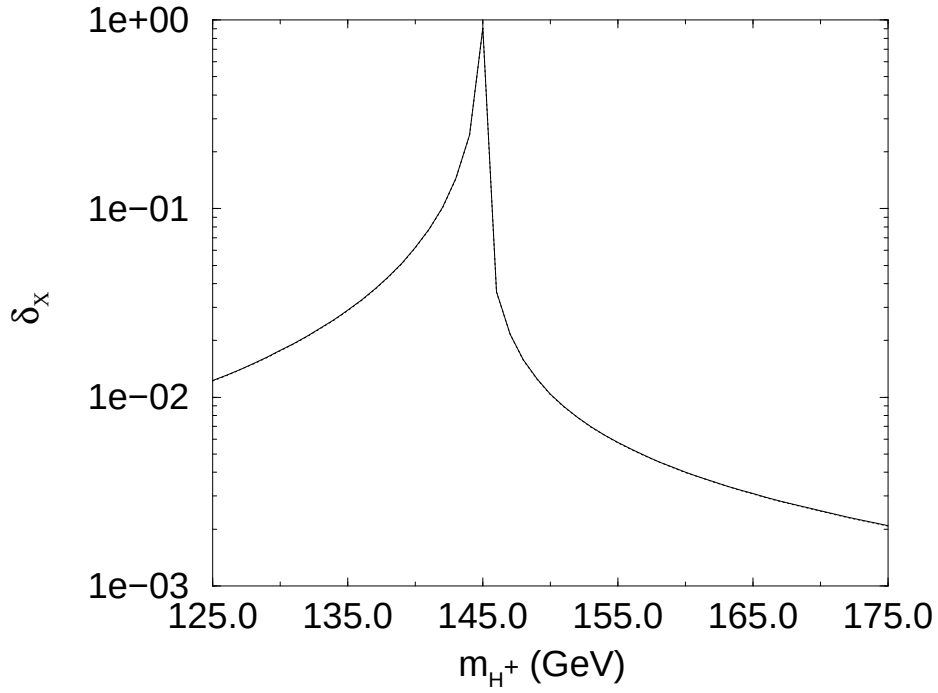
1e+00
1e−01
1e−02
1e−03
δ_X
125.0
135.0
145.0
155.0
165.0
175.0
m_{H^+} (GeV)

(a)

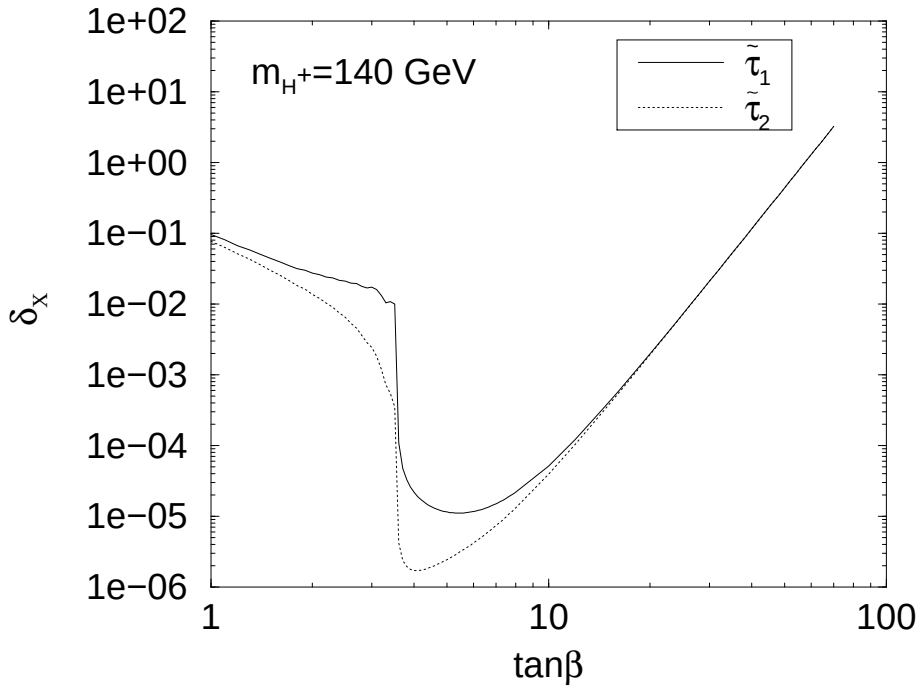
1e+02
1e+01
1e+00
1e−01
1e−02
1e−03
1e−04
1e−05
1e−06
δ_X
m_{H^+}=140 GeV
$\tilde{\tau}_1$
$\tilde{\tau}_2$
1
10
100
tanβ

(b)

Fig. 18

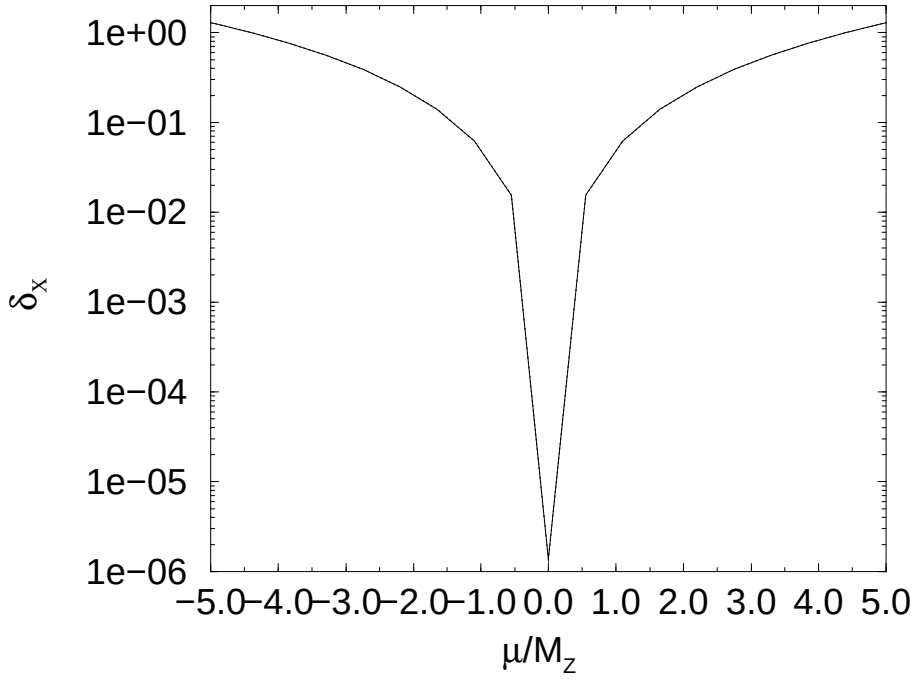
1e+00
1e−01
1e−02
1e−03
1e−04
1e−05
1e−06
δx
−5.0 −4.0 −3.0 −2.0 −1.0 0.0 1.0 2.0 3.0 4.0 5.0
μ/Mz

(c)

Fig. 18